

1 **Preexisting memory CD4 T cells in naïve individuals confer robust**
2 **immunity upon hepatitis B vaccination**

3 **Running title: Preexisting memory T cells confer immunity to vaccination**

4 **George Elias**^{1,2%}, **Pieter Meysman**^{2,3,4%}, **Esther Bartholomeus**^{2,5%}, **Nicolas De Neuter**
5 ^{2,3,4}, **Nina Keersmaekers**^{2,6}, **Arvid Suls**^{2,5}, **Hilde Jansens**⁷, **Aisha Souquette**⁸, **Hans De Reu**
6 ^{1,9}, **Evelien Smits**^{1,9}, **Eva Lion**^{1,9}, **Paul G. Thomas**⁸, **Geert Mortier**^{2,5}, **Pierre Van Damme**
7 ^{2,10}, **Philippe Beutels**^{2,6}, **Kris Laukens**^{2,3,4%}, **Viggo Van Tendeloo**^{1,11%}, **Benson Ogunjimi**
8 ^{2,6,12,13%}

9
10 **% = equal contribution**

11 ¹Laboratory of Experimental Hematology (LEH), Vaccine and Infectious Disease Institute, University of Antwerp,
12 Antwerp, Belgium.

13 ²Antwerp Unit for Data Analysis and Computation in Immunology and Sequencing (AUDACIS), Antwerp, Belgium.

14 ³Adrem Data Lab, Department of Mathematics and Computer Science, University of Antwerp, Antwerp, Belgium.

15 ⁴Biomedical Informatics Research Network Antwerp (biomina), University of Antwerp, Antwerp, Belgium.

16 ⁵Department of Medical Genetics, University of Antwerp/Antwerp University Hospital, Antwerp, Belgium

17 ⁶Centre for Health Economics Research & Modeling Infectious Diseases (CHERMID), Vaccine & Infectious Disease
18 Institute (VAXINFECTIO), University of Antwerp, Antwerp, Belgium

19 ⁷Department of Clinical Microbiology, Antwerp University Hospital, Antwerp, Belgium

20 ⁸Department of Immunology, St. Jude Children's Research Hospital, Memphis, Tennessee, USA

21 ⁹Center for Cell Therapy and Regenerative Medicine, Antwerp University Hospital, Antwerp, Belgium

22 ¹⁰Centre for the Evaluation of Vaccination (CEV), Vaccine and Infectious Disease Institute, University of Antwerp,
23 Antwerp, Belgium.

24 ¹¹Janssen Research & Development, Immunosciences WWDA, Johnson & Johnson, Beerse, Belgium

25 ¹²Antwerp Center for Translational Immunology and Virology (ACTIV), Vaccine and Infectious Disease Institute,
26 University of Antwerp, Antwerp, Belgium

27 ¹³Department of Paediatrics, Antwerp University Hospital, Antwerp, Belgium.

28 Corresponding authors: George Elias, Benson Ogunjimi

29 **E-mail address:**

30 george.elias@student.uantwerpen.be, benson.ogunjimi@uantwerp.be

31 Laboratory of Experimental Hematology (LEH), Vaccine and Infectious Disease Institute,
32 University of Antwerp, Universiteitsplein 1, 2610 Antwerp, Belgium

33

34

35

36

37 **Footnotes**

38 This work was funded by

39 1. University of Antwerp [BOF Concerted Research Action (PS ID 30730) Methusalem
40 funding; Industrial Research Fund SBO].

41 2. Research Foundation Flanders (1861219N grant to B. Ogunjimi and FWO SB grant to N.
42 De Neuter).

43 3. ALSAC at St. Jude Children's Research Hospital and by HSN272201400006C and
44 R01AI107625 from the National Institute of Allergy and Infectious Disease.

45

46

47 **Summary**

48 Antigen recognition through the T cell receptor (TCR) $\alpha\beta$ heterodimer is one of the primary
49 determinants of the adaptive immune response. Vaccines activate naïve T cells with high
50 specificity to expand and differentiate into memory T cells. However, antigen-specific memory
51 CD4 T cells exist in unexposed antigen-naïve hosts. In this study, we use high-throughput
52 sequencing of memory CD4 TCR β repertoire and machine learning to show that individuals with
53 preexisting vaccine-reactive memory CD4 T cell clonotypes elicited earlier and higher antibody
54 titers and mounted a more robust CD4 T cell response to hepatitis B vaccine. In addition,
55 integration of TCR β sequence patterns into a hepatitis B vaccine specific model can predict
56 which individuals will have an early and more vigorous vaccine-elicited immunity. Thus, the
57 presence of preexisting memory T clonotypes has a significant impact on immunity and can be
58 used to predict immune responses to vaccination.

59

60

61

62

63

64 **Keywords**

65 CD4 T cell, T cell receptor, TCR sequencing, TCR repertoire, immune repertoire sequencing,
66 vaccination

67

68

69 **Introduction**

70 Antigen recognition through the T cell receptor (TCR) is one of the key determinants of the
71 adaptive immune response (Rudolph et al., 2006). Antigen presentation via major
72 histocompatibility complex (MHC) (encoded by HLA genes), together with the right
73 costimulatory and cytokine signals, are responsible for T cell activation (Curtsinger and
74 Mescher, 2010; Esensten et al., 2016). In this system, every T cell receptor (TCR) $\alpha\beta$
75 heterodimer imparts specificity for a peptide-MHC (pMHC) complex. A highly diverse TCR
76 repertoire ensures that an effective T cell response can be mounted against pathogen-derived
77 peptides (Turner et al., 2009). High TCR $\alpha\beta$ diversity is generated through V(D)J recombination
78 at the complementary-determining region 3 (CDR3) of TCR α and TCR β chains, accompanied
79 with junctional deletions and insertions of nucleotides, further adding to the diversity (Kragel,
80 2009).

81 Vaccines activate naïve T cells with high specificity to vaccine-derived peptides and induce their
82 expansion and differentiation into effective and multifunctional T cells. This is followed by a
83 contraction phase from which surviving cells constitute a long-lived memory T cell pool that
84 allows for a quick and robust T cell response upon a second exposure to the pathogen (Farber et
85 al., 2014). However, recent work has shown that a prior pathogen encounter is not a prerequisite
86 for the formation of memory T cells and that CD4 T cells with a memory phenotype can be
87 found in antigen-naïve individuals (Su et al., 2013). The existence of memory-like CD4 T cells
88 in naïve individuals (Sewell, 2012) can be explained by molecular mimicry, as the encounter
89 with environmentally-derived peptides activates cross-reactive T cells due to the highly
90 degenerate nature of the CD4 T cell recognition of peptide-MHC complex (Wilson et al., 2004).
91 Indeed, work that attempted to replicate the history of human pathogen exposure in mice has

92 shown that sequential infections altered the immunological profile and remodeled the immune
93 response to vaccination (Reese et al., 2016). The existence of memory CD4 T cells specific to
94 vaccine-derived peptides in unexposed individuals might confer an advantage in vaccine-induced
95 immunity. In the present study we used high-throughput sequencing to profile the memory CD4
96 TCR β repertoire of healthy adults before and after administration of a hepatitis B vaccine to
97 investigate the impact of preexisting memory CD4 T cells on the immune response to the
98 vaccine. Based on anti-hepatitis B surface (anti-HBs) antibody titers over 365 days, vaccinees
99 were grouped into early, late and non-converters. Our data reveals that individuals with
100 preexisting vaccine-specific CD4 T cell clonotypes in the memory CD4 compartment had earlier
101 emergence of antibodies and mounted a more vigorous CD4 T cell response to the vaccine.
102 Moreover, we identify a set of vaccine-specific TCR β sequence patterns which can be used to
103 predict which individuals will have an early and more vigorous response to hepatitis B vaccine.

104

105

106

107

108

109

110

111

112

113

114

115 **Results:**

116 **Vaccinee cohort can be classified into three groups**

117 Out of 34 vaccinees, 21 vaccinees seroconverted (an anti-HBs titer above 10 IU/ml was
118 considered protective (Keating and Noble, 2003)) at day 60 and were classified as early-
119 converters; 9 vaccinees seroconverted at day 180 or day 365 and were classified as late-
120 converters; remaining 4 vaccinees had an anti-HBs antibody titer lower than 10 IU/ml at all time
121 points following vaccination and were classified as non-converters (**Fig. 1** and **Fig. S2a**).

122 Members of *Herpesviridae* family might alter immune responses to vaccines (Furman et al.,
123 2015). We found no significant differences in CMV, EBV or HSV seropositivity between the
124 three groups in our cohort (**Fig. S2b**). Early-converters were slightly younger than late-
125 converters and non-converters were notably younger than both early and late converters (**Fig.**
126 **S2c**).

127 128 **Memory CD4 T cell repertoire in early-converters decreases in clonality following** 129 **vaccination**

130 A genomic DNA-based TCR β sequence dataset of memory CD4 T cells isolated from peripheral
131 blood was generated from a cohort of 33 healthy vaccinees (see *Methods* for details) right before
132 vaccination (day 0) and 60 days after administration of the first dose of hepatitis B vaccine (30
133 days after administration of the second vaccine dose).

134 Between 4.54×10^4 and 3.92×10^5 productive TCR β sequence reads were obtained for each
135 vaccinee at each time point (**Fig. S3a**). Between 30,000 and 90,000 unique TCR β sequences
136 were sequenced for each vaccinee at each time point (**Fig. S3b**). As expected, considering the

137 extremely diverse memory CD4 T cell repertoire (Klarenbeek et al., 2010), less than 20% of the
138 TCR β sequences is shared between the time points for each vaccinee (**Fig. S3c**).

139

140 The diversity of the memory CD4 T cell repertoire of each vaccinee at the two time points was
141 explored. Even though the number of unique clones in the memory CD4 TCR β repertoire
142 remained stable in between the two time points, we detected a significant increase in the TCR β
143 repertoire Shannon's entropy for early-converters (**Fig. 2a**) (P value = 0.042), but not late-
144 converters, suggesting that the memory CD4 T cell repertoires of early-converters have become
145 less clonal, despite the number of distinct TCR β sequences not changing significantly.

146

147 **Unique vaccine-specific TCR β sequences are trackable within memory CD4 T cell**
148 **repertoire and increase following vaccination**

149 Peripheral blood mononuclear cells from day 60 were labeled with carboxyfluorescein
150 succinimidyl ester (CFSE) and stimulated with a pool of peptides spanning hepatitis B (HB)
151 surface antigen (HBsAg). After day 7 of *in vitro* expansion, we sorted CFSE^{low} CD4 T cells
152 (Becattini et al., 2015) and extracted mRNA for quantitative assessment of HBsAg-specific
153 TCR β clonotypes by sequencing (see *Methods* for details), allowing for the tracking of vaccine-
154 specific TCR β within memory CD4 T cell repertoire over the two times points, based on CDR3 β
155 amino acid sequence mapping.

156 We detected a significant increase in the frequency of unique HBsAg-specific TCR β sequences
157 at day 60 post-vaccination compared to pre-vaccination (mean increase = 96.5%, 95% CI = 56.7
158 - 170%) (**Fig. 2b** and **S3d**). Moreover, this increase was larger for early-converters (mean =
159 132.1%, 95% CI = 76.4 - 238.2%) than late-converters (mean = 22.1%, 95% CI = 5.9 - 50.1%).

160 For non-converters the mean was 81.6% (95% CI: [42.7% - 110.6%]). A Wilcoxon test shows
161 that the difference between the increase for the early converters and late converters had a P value
162 of 0.04909.

163 As HBsAg-specific TCR β sequences were already detected in the memory CD4 T cell repertoire
164 prior to vaccination, we sought to determine whether the vaccination results in an expansion of
165 those sequences. Using the abundance of vaccine-specific TCR β sequences within the memory
166 CD4 T cell repertoire, the data does not support a vaccine-induced expansion of preexisting
167 vaccine-specific TCR β sequences (**Fig. S3e**). Thus, although we see a rise in the number of
168 vaccine-specific TCR β clonotypes from day 0 to day 60, this cannot be attributed to an
169 expansion of preexisting TCR β clonotypes but rather the recruitment of new TCR β clonotypes
170 (presumably from the naïve T cell compartment), as visualized for one vaccinee in **Fig. 2c**.

171 It makes sense to not only look at the difference in vaccine-specific TCR β sequences between
172 time points, but also explore whether there are differences in the proportion of HBsAg-specific
173 clones in the memory repertoire between early-converters, late-converters and non-converters
174 after vaccination. In this case, as we aim for a between-vaccinees comparison (in contrast to the
175 within-vaccinees timepoint comparison), we normalize by the number of HBsAg-specific TCR β
176 found for each vaccinee. Thus, the values are different from those reported before. From this
177 analysis, it can be concluded that there is a difference in HBsAg-specific TCR β at day 60
178 between the three groups (**Fig. 2d**) (ANOVA P value = 0.00238). A Wilcoxon test between
179 early-converters and other vaccinees shows a significant P value of 0.000473, indicating that
180 early-converters have a higher relative frequency of vaccine-specific TCR β sequences present in
181 their memory CD4 T cell repertoire at day 60 compared to vaccinees from the two other groups
182 in the cohort.

183

184

185 **HBsAg single peptide-specific TCR β identification allows predictive modelling of early**
186 **converters prior to vaccination**

187 To quantify the T cell response at the level of individual peptides that make up the HBsAg, a
188 matrix peptide pool covering 54 overlapping peptides of the HBsAg was used to extract peptide-
189 specific T-cells using a CD40L/CD154 activation-induced marker (AIM) assay (see *Methods* for
190 details, **Fig. S4**). The top 6 peptides for each individual were selected for TCR sequencing after a
191 CFSE assay (**Supplementary Table 2**). In this manner, TCR β sequences were identified for T-
192 cells reactive against 44 single HBsAg peptides. These were not uniformly distributed across the
193 HBsAg amino acid sequence, with the most prominent epitopes covering the regions 1-15, 129-
194 144, 149-164, 161-176, 181-200, 213-228. For each of those regions, more than 10 individuals
195 had a strong T-cell response and more than 150 unique TCR β sequences could be identified (**Fig.**
196 **3a**).

197 These peptide-specific TCR β sequences can be utilized in a peptide-TCR interaction classifier to
198 identify other TCR β that are likely to react against same HBsAg epitopes, as it has been shown
199 that similar TCR β sequences tend to target the same epitopes (Meysman et al., 2018; De Neuter
200 et al., 2018). These classifications were integrated into a model which outputs a **ratio R_{hbs}** for
201 any TCR β repertoire representing the amount of HBsAg peptide-specific clonotypes. **R_{hbs}** is
202 based on the frequency of putative peptide-specific TCR β divided by a normalization term for
203 putative false positive predictions due to bystander activations in the training data set. This
204 model applied to the memory repertoire at day 60 shows that early-converters tend to have a
205 higher frequency of putative HBsAg peptide-specific TCR β , while late-converters tend to have
206 relatively more false positive hits (**Fig. 3b**). Thus, the defined ratio **R_{hbs}** shows significant
207 difference between early the late-converters at day 60 (one-sided Wilcoxon-test P value= 0.0313,

208 **Fig. 3c**). Furthermore, calculating R_{hbs} on the memory repertoires prior to vaccination (day 0)
209 shows a similar difference (one-sided Wilcoxon-test P value= 0.0010, **Fig. 3d**). In this manner,
210 R_{hbs} has predictive potential and can be used as a classifier to distinguish early from late-
211 converters prior to vaccination (**Fig. 3e**), with an AUC of 0.825 (95% CI: 0.657 – 0.994) in a
212 leave-one-out cross validation setting. To account for the age variable, a model in which age-
213 matched vaccinees were included from early and late-converters returned a similar ROC curve
214 (**Fig. S3f**).

215 While R_{hbs} is able to differentiate between early-and late-converters, it seems to be worse at
216 distinguishing non-converters. This is mainly due to a single non-converter vaccinee (H21) with
217 a high R_{hbs} , signifying a high number of putative HBsAg peptide-specific TCR β in their memory
218 repertoire.

219

220 **Vaccine-specific conventional and regulatory memory CD4 T cells induced in early-** 221 **converters**

222 After showing evidence for the existence of vaccine-specific TCR β sequences pre-vaccination
223 and that individuals with a higher number of HBsAg peptide-specific clonotypes had earlier
224 seroconversion, we attempted to link this observation to differences in vaccine-specific CD4 T
225 cells responses using CD4 T cell assays. As T_{REG} cells might suppress vaccine-induced immune
226 responses (Brezar et al., 2016), we used activation markers CD40L (CD154) and 4-1BB
227 (CD137) to help delineate the conventional (T_{CON}) and regulatory (T_{REG}) phenotypes of activated
228 CD4 T cells. In this scheme, after 6 hours of antigen stimulation, CD40L⁺4-1BB⁻ can be used as
229 a signature for antigen-specific CD4 T_{CON} cells, as opposed to CD40L⁻4-1BB⁺ signature for
230 antigen-specific CD4 T_{REG} cells (Elias et al., 2020; Schoenbrunn et al., 2012).

231 Additionally, we added CD25 and CD127 to better identify T_{REG} cells (Liu et al., 2006; Seddiki
232 et al., 2006) and CXCR5 to further distinguish circulatory T follicular helper cells (cT_{FH}) and
233 circulatory T follicular regulatory cells (cT_{FR}) (Bentebibel et al., 2011; Fonseca et al., 2017).
234 Using the converse expression of CD40L and 4-1BB, CD40L⁺4-1BB⁻ and CD40L⁻4-1BB⁺ CD4
235 T cells had a T_{CON} and T_{REG} phenotype, respectively, as shown by the expression of CD25 and
236 CD127 (**Fig. S5a** and **b**), and validate their use for the distinction of activated T_{CON} and T_{REG}
237 cells as has been reported before (Schoenbrunn et al., 2012).
238 We detected a significant increase in the frequency of CD40L⁺4-1BB⁻ and CD40L⁻4-1BB⁺
239 memory CD4 T cells at day 60 in our cohort (**Fig. 4a**) that correlated positively with the increase
240 in antibody titer between day 0 and day 365 (**Fig. 4b** and **Fig. S6**). Upon a closer look, the
241 induction of both signatures of vaccine-specific memory CD4 T cells was only true for early-
242 converters (**Fig. 4c**, see **Fig. S7a** for non-converters and **Fig. S7b** for vaccine-specific CD4 T
243 cells) while late-converters did not show a detectable memory CD4 T cell response. Although a
244 subset of both early and late-converters had detectable memory CD4 T cell responses prior to
245 vaccination, we observed no significant differences in the frequencies of CD40L⁺4-1BB⁻ and
246 CD40L⁻4-1BB⁺ memory CD4 T cells between the two groups at day 0 (**Fig. 4d**).
247 Collectively, flow cytometry data reveal that the expression of CD40L and 4-1BB in our ex vivo
248 assay is consistent with our serological data and reflects the lack of seroconversion at day 60 in
249 late-converters. However, it does not support the existence of more vaccine-specific memory
250 CD4 T cells in early-converters prior to vaccination.

251

252

253 **Predictive capacity of TCR β repertoire holds true for CD4 T_{CON} immune response**

254 Response groups used thus far were established based on the dynamics of anti-HBs titers
255 following vaccination. However, response groups can be defined based on the data of antigen-
256 specificity from the ex vivo CD4 T cell assay. Redoing the analysis with \mathbf{R}_{hbs} to predict the
257 frequency of CD40L⁺4-1BB⁻ and CD40L⁻4-1BB⁺ memory CD4 T cells at three different times
258 points (days 60, 180 and 365) shows that the \mathbf{R}_{hbs} is a good classifier in a leave-one-out cross
259 validation for HBsAg-specific memory CD4 T cells with a T_{CON} signature identified at day 60
260 post-vaccination (**Fig. 4e and f**) and that is to a large extent lacking for delayed time points.

261

262

263

264

265 **An expanded subset of 4-1BB⁺CD45RA⁻ T_{REG} cells is a prominent feature of late-**
266 **converters**

267 In order to detect any distinct signatures of early and late-converters, we analyzed pre-
268 vaccination flow cytometry data to examine major CD4 T cell subsets; T_H, T_{REG}, cT_{FH} and cT_{FR}
269 cells. Using manual gating in which regulatory T cells (T_{REG}) were defined as viable
270 CD3⁺CD4⁺CD8⁻CD25⁺CD127⁻CXCR5⁻ and were further divided into CD45RA⁺ and CD45RA⁻
271 T_{REG} cells, we identified a significantly higher frequency of 4-1BB⁺ CD45RA⁻ T_{REG} cells in late-
272 converters compared to early-converters (**Fig. 5a and Fig. S8**).

273 T_{REG} cells showed higher 4-1BB expression compared to T_H, cT_{FH} and cT_{FR} cells (**Fig. 5b**) and
274 within T_{REG} subset, CD45RA⁻ T_{REG} cells showed significantly higher expression of 4-1BB,
275 accompanied with a higher expression of CD25, compared to CD45RA⁺ T_{REG} cells (**Fig. 5c**). In
276 this scheme, CD45RA⁻ T_{REG} can be divided into 4-1BB⁺CD25^{high} and 4-1BB⁻CD25^{int} subsets. It
277 is worth noting here that no differences were detected in the frequency of CD45RA⁻ or
278 CD45RA⁺ T_{REG} cells within CD4 T cell compartment between the two groups (**Fig. 5d**), and that
279 the composition of T_{REG} compartment that is distinct between the two groups (**Fig. 5e**).

280 In summary, an expanded subset of 4-1BB⁺CD45RA⁻ T_{REG} cells pre-vaccination is a prominent
281 feature of a delayed and modest immune response to hepatitis B vaccine in our cohort.

282

283 **Discussion**

284 In this study, we used high-throughput TCR β repertoire profiling and *ex vivo* T cell assays to
285 characterize memory CD4 T cell repertoires before and after immunization with hepatitis B
286 vaccine, an adjuvanted subunit vaccine, and tracked vaccine-specific TCR β clonotypes over two
287 time points. As antigen-naïve adults were found to have an unexpected abundance of memory-

288 phenotype CD4 T cells specific to viral antigens (Su and Davis, 2013; Su et al., 2013), we sought
289 to investigate the influence that preexisting memory CD4 T cells can have on vaccine-induced
290 immunity.

291 Commercially available HBV vaccines produces a robust and long-lasting anti-HBs response,
292 and protection is provided by induction of an anti-HBs (antibody against HBV surface antigen)
293 titer higher than 10 mIU/mL after a complete immunization schedule of 3 doses (Meireles et al.,
294 2015). However, 5-10% of healthy adult vaccinees fail to produce protective titers of anti-HBs
295 and can be classified as non-responders (Meireles et al., 2015). In our cohort, 13 vaccinees did
296 not seroconvert by day 60 (30 days following administration of the second vaccine dose), as
297 determined by antibody titer. Out of this group, 9 vaccinees seroconverted by day 180 or day
298 365, referred to here as late-converters, and 4 vaccinees did not seroconvert, referred to here as
299 non-converters.

300 A hallmark of adaptive immunity is a potential for memory immune responses to increase in
301 both magnitude and quality upon repeated exposure to the antigen (Sallusto et al., 2010). Our
302 systems immunology data supports the theory that preexisting memory CD4 T cell TCR β
303 sequences specific to HBsAg, the antigenic component of the current hepatitis B vaccine, predict
304 which individuals will mount an early and more vigorous immune response to the vaccine as
305 evidenced by a higher fold change in anti-HBs antibody titer and a more significant induction of
306 antigen-specific CD4 T cells. It is postulated that preexisting memory CD4 T cell clonotypes are
307 generated due to the highly degenerate nature of T cell recognition of antigen/MHC and are
308 cross-reactive to environmental antigens (Sewell, 2012). For example, preexisting memory CD4
309 T cells are well-established in unexposed HIV-seronegative individuals, although at a
310 significantly lower magnitude than HIV-exposed seronegative individuals (Campion et al., 2014;

311 Ritchie et al., 2011), and were likely primed by exposure to environmental triggers or the human
312 microbiome.

313 We and others have shown before that the TCR β repertoire of CD4 T cells encodes the antigen
314 exposure history of each individual and that antigen-specific TCR β sequences could serve to
315 automatically annotate the infection or exposure history (DeWitt et al., 2018; Emerson et al.,
316 2017; de Neuter et al., 2018). In this study, we show that similar principles can be used to study
317 vaccine responsiveness. Specifically, the recruitment of novel vaccine-specific T-cell clonotypes
318 into memory compartment following vaccination can be tracked by examining the CD4 memory
319 TCR β repertoire over time. While we observed no increase in the frequency of the vaccine-
320 specific memory T-cells, as the time point may have missed the peak of the clonal expansion of
321 effector CD4 T cells as was reported before (Blom et al., 2013; Kohler et al., 2012; Pogorelyy et
322 al., 2018), a significant rise in the number of unique vaccine-specific T-cell clonotypes was
323 detected. This observation is consistent with earlier studies of T cell immune repertoire that
324 showed that antigen-specific TCR β sequences do not always overlap with those sequences that
325 increase in frequency after infection or vaccination (DeWitt et al., 2015). More interestingly,
326 individuals with the earlier and more robust response against the vaccine, had a telltale antigen-
327 specific signature in their memory TCR β repertoire prior to vaccination, despite the lack of
328 HBsAg antibodies or prior vaccination history.

329

330 Detection of this vaccine-specific signature was possible due to the development of a novel
331 predictive model that used epitope-specific TCR β sequences from one set of individuals to make
332 predictions about another. A correction factor was needed to account for the occurrence of
333 bystander activated T cells within the original epitope-specific TCR β sequences. Indeed, in those

334 vaccinees without a positive antibody titer at day 60, putative vaccine-specific T cells might be
335 induced due to bystander activation. This was supported by predictions using the TCRex tool
336 (Gielis et al., 2019), which matched these TCR sequences to common viral or other epitopes. It is
337 of note that these TCR β sequences are matched with CD8 T cell epitopes, while they originate
338 from isolated CD4 T cells. This is likely due to the great similarity between the TCR β sequences
339 of CD4 and CD8 T cells as noted in prior research (Meysman et al., 2018).

340

341 However, our in vitro antigen-specificity data, using an assay that enables discrimination of
342 T_{CON} and T_{REG} cells using the converse expression of the activation markers CD40L and 4-1BB
343 (Frentsch et al., 2005; Schoenbrunn et al., 2012), failed to show a significant difference in
344 preexisting antigen-specific CD4 T cells between early and late-converters prior to vaccine
345 administration. It is plausible that the signal is below the detection limit of the assay and that
346 more sensitive assays that require pre-enrichment of CD40L⁺ and 4-1BB⁺ T cells (using
347 magnetic beads) (Bacher et al., 2013) or cultured ELISpot assay (Reece et al., 2004) are needed
348 to capture preexisting vaccine-specific memory CD4 T cells directly from human peripheral
349 blood. Another plausible explanation is that our activation proteins, CD40L and 4-1BB, might be
350 unsuitable to detect preexisting memory CD4 T cells but this is unlikely as both proteins have
351 been used successfully in similar studies (Bacher et al., 2014b, 2014a). A different explanation
352 may be that the diversity of preexisting antigen-specific CD4 T clonotypes as determined by
353 TCR β sequencing is not reflected in the quantitative measurements of the fractional cell counts.
354 A similar disconnect between clonotype diversity underlying vaccine response and cell counts in
355 an ELISPOT setting was observed in Galson et al (Galson et al., 2016).

356

357 T_{REG} cells represent about 5 – 10% of human CD4 T cell compartment and are identified by the
358 constitutive surface expression of CD25, also known as IL-2 receptor α subunit (IL-2Ra), and the
359 nuclear expression of forkhead family transcription factor 3 (Foxp3), a lineage specification
360 factor of T_{REG} cells (Rudensky, 2011). Regulatory memory T cells play a role in the mitigation of
361 tissue damage induced by effector memory T cells during protective immune responses, resulting
362 in a selective advantage against pathogen-induced immunopathology (Garner-Spitzer et al.,
363 2013; Lanteri et al., 2009; Lin et al., 2018; Lovelace and Maecker, 2018). Several studies have
364 identified CD4 T_{REG} cells with specificity to pathogen-derived peptides in murine models and
365 showed evidence for an induced expansion of T_{REG} cells followed by an emergence and a long-
366 term persistence of T_{REG} cells with a memory phenotype and potent immunosuppressive
367 properties (Lin et al., 2018; Sanchez et al., 2012). Blom et al. reported a significant and transient
368 activation of T_{REG} cells (identified by upregulation of CD38 and Ki67) in humans 10 days after
369 administration of live attenuated yellow fever virus 17D vaccine (Blom et al., 2013). The
370 induction of vaccine-specific T_{REG} cells in our cohort is unexpected and the role it might play in
371 vaccine-induced immunity warrants further investigation.

372

373 The association of an expanded 4-1BB⁺ CD45RA⁻ T_{REG} subset with a delayed immune response
374 to hepatitis B vaccine was not described before. Miyara et al. showed that blood contains two
375 distinct subsets of stable and suppressive T_{REG} cells: resting T_{REG}, identified as
376 FOXP3^{low}CD45RA⁺ CD4 T cells, and activated T_{REG}, identified as FOXP3^{high}CD45RA⁻ CD4 T
377 cells. They further noted that activated T_{REG} cells constitute a minority subset within cord blood
378 T_{REG} cells and increase gradually with age (Miyara et al., 2009). As activated T_{REG} cells were
379 shown to have an increased expression of proteins indicative of activation, including ICOS and

380 HLA-DR (Booth et al., 2010; Ito et al., 2008; Mason et al., 2015; Miyara et al., 2009; Mohr et
381 al., 2018), it might be the case that an upregulation of 4-1BB is one more feature of this
382 population or a subset thereof. Moreover, T_{REG} cells in mice were shown to modulate T_{FH}
383 formation and GC B cell responses and to diminish antibody production in a CTLA-4 mediated
384 suppression (Wing et al., 2014). Interestingly, CD45RA⁻ T_{REG} cells were shown to be more rich
385 in preformed CTLA-4 stored in intracellular vesicles compared to CD45RA⁺ T_{REG} cells (Miyara
386 et al., 2009).

387 4-1BB was shown to be constitutively expressed by T_{REG} cells (McHugh et al., 2002) and that 4-
388 1BB⁺ T_{REG} cells are functionally superior to 4-1BB⁻ T_{REG} cells in both contact-dependent and
389 contact-independent immunosuppression (Kachapati et al., 2012). 4-1BB⁺ T_{REG} cells are the
390 major producers of the alternatively-spliced and soluble isoform of 4-1BB among T cells
391 (Kachapati et al., 2012). 4-1BB was shown before to be preferentially expressed on T_{REG} cells
392 compared with other non-regulatory CD4 T cell subsets (McHugh et al., 2002) and that 4-1BB-
393 costimulation induces the expansion of T_{REG} cells both in vitro and in vivo (Zheng et al., 2004).
394 Moreover, agonistic anti-4-1BB mAbs have been shown to abrogate T cell-dependent antibody
395 responses in vivo (Mittler et al., 1999) and to ameliorate experimental autoimmune
396 encephalomyelitis by skewing the balance against T_H17 differentiation in favor of T_{REG}
397 differentiation (Kim et al., 2011). It is plausible that the expansion 4-1BB⁺CD45RA⁻ T_{REG} cells
398 in late-converters is involved in the suppression of GC vaccine-specific T_{FH} cells and the ensuing
399 antibody response in our cohort, but this remains speculative and further research is warranted.

400

401 It is enticing to speculate that the preexisting memory CD4 T cells result from the complex
402 interplay between cellular immunity and the human microbiome. A role for the microbiota in

403 modulating immunity to viral infection was suggested in 1960's (Robinson and Pfeiffer, 2014),
404 and since then we gained better understanding of the impact of the various components of the
405 microbiota including bacteria, fungi, protozoa, archaea and viruses on the murine and human
406 immune systems (Winkler and Thackray, 2019).

407 Viral clearance of hepatitis B virus infection depends on the age of exposure and neonates and
408 young children are less likely to spontaneously clear the virus (Yuen et al., 2018). Han-Hsuan et
409 al. have shown evidence in mice that this age-dependency is mediated by gut microbiota that
410 prepare the liver immunity system to clear HBV, possibly via a TLR4 signaling pathway (Chou
411 et al., 2015). In this study, young mice that have not reached an equilibrium in the gut
412 microbiota, exhibited prolonged HBsAg persistence, impaired anti-HBs antibody production, and
413 limited Hepatitis B core antigen (HBcAg)-specific IFN γ ⁺ splenocytes. More recently, Tingxin et
414 al. provided evidence for a critical role of the commensal microbiota in supporting the
415 differentiation of GC B cells, through follicular T helper (T_{FH}) cells, to promote the anti-HBV
416 humoral immunity (Wu et al., 2019).

417

418 Our study bears some intrinsic limitations. A major drawback is the restricted number of days at
419 which TCR β repertoire was profiled, as vaccine-specific perturbations within the repertoire may
420 occur at different time points for early, late and non-converters. Additionally, more in-depth
421 characterization and functional studies on 4-1BB⁺CD45RA⁻ T_{REG} cells could have helped shed
422 more light on the role they play in vaccine-induced immunity. Future studies in larger cohorts
423 and with a more comprehensive TCR β repertoire profiling and CD4 T cells immunophenotyping
424 are required to validate our findings.

425

426 In conclusion, our analysis of the memory CD4 T cell repertoire has uncovered a role for
427 preexisting memory CD4 T cells in naïve individuals in mounting an earlier and more vigorous
428 immune response to hepatitis B vaccine and argue for the utility of pre-vaccination TCR β
429 repertoire in the prediction of vaccine-induced immunity. Moreover, we identify a subset of 4-
430 1BB⁺ memory T_{REG} cells that is expanded in individuals with delayed immune response to the
431 vaccine, which might further explain the heterogeneity of response to hepatitis B vaccine.

432

433

434 **AUTHOR CONTRIBUTIONS**

435 Conception: PM, BO

436 Design: GE, PM, EB, AS, GM, PVD, PB, KL, VVT, BO

437 Experiments: GE, PM, EB, NDN, HJ, AS

438 Data-analysis: GE, PM, NDN, BO

439 Supervision: HDR, EL, PT, GM, PVD, PB, KL, VVT, BO

440 First draft: GE, PM, BO

441 Contributed to the paper: all authors

442

443 **COMPETING FINANCIAL INTERESTS**

444 Parts of the contents of this manuscript form the topic of patent EPO 19159931.5.

445 VVT is an employee of Johnson & Johnson since 1/11/2019 and remains currently employed at

446 the University of Antwerp.

447

448 **Methods**

449 **Human study design and clinical samples.** A total of 34 healthy individuals (20-29y: 10, 30-
450 39y: 7, 40-49y: 16, 50+y: 1) without a history of HBV infection or previous hepatitis B
451 vaccination were recruited in this study after obtaining written informed consent. Individuals
452 were vaccinated with a hepatitis B vaccine by intramuscular (m. deltoideus) injection (Engerix-
453 B[®] containing 20 µg dose of alum-adjuvanted hepatitis B surface antigen, GlaxoSmithKline) on
454 days 0 and 30 (and on day 365). At days 0 (pre-vaccination), 60, 180 and 365, peripheral blood
455 samples were collected on spray-coated lithium heparin tubes, spray-coated K2EDTA
456 (dipotassium ethylenediamine tetra-acetic acid) tubes and serum tubes (Becton Dickinson, NJ,
457 USA).

458
459 **Peripheral blood mononuclear cells.** Peripheral blood mononuclear cells (PBMC) were
460 isolated by Ficoll-Paque Plus gradient separation (GE Healthcare, Chicago, IL, USA). Cells were
461 stored in 10% dimethyl sulfoxide in fetal bovine serum (Thermo Fisher Scientific, Waltham,
462 MA, USA). After thawing and washing cryopreserved PBMC, cells were cultured in AIM-V
463 medium that contained L-glutamine, streptomycin sulfate at 50 µg/ml, and gentamicin sulfate at
464 10 µg/ml (Thermo Fisher Scientific, Waltham, MA, USA) and supplemented with 5% human
465 serum (One Lambda, Canoga Park, CA, USA).

466
467 **Serology and complete blood count.** Serum was separated and stored immediately at – 80°C
468 until time of analysis. Anti-HBs antibody was titrated in serum from day 0, 60, 180 and 365
469 using Roche Elecsys[®] Anti-HBs antibody assay on an Elecsys[®] 2010 analyzer (Roche, Basel,

470 Switzerland). An anti-HBs titer above 10 IU/ml was considered protective (Keating and Noble,
471 2003).

472 Serum IgG antibodies to Cytomegalovirus (CMV), Epstein–Barr virus viral-capsid antigen
473 (EBV-VCA), and Herpes Simplex virus (HSV)-1 and 2 were determined using commercially
474 available sandwich ELISA kits in accordance with the manufacturer’s instructions.

475 A complete blood count including leukocyte differential was run on a hematology analyzer
476 (ABX MICROS 60, Horiba, Kyoto, Japan).

477

478 **Sorting of memory CD4 T cells.** Total CD4 T cells were isolated by positive selection using
479 CD4 magnetic microbeads (Miltenyi Biotech, Bergisch Gladbach, Germany). Memory CD4 T
480 cells were sorted after gating on single viable CD3⁺CD4⁺CD8⁻CD45RO⁺ cells. The following
481 fluorochrome-labeled monoclonal antibodies were used for staining: CD3-PerCP (BW264/56)
482 (Miltenyi Biotech), CD4-APC (RPA-T4) and CD45RO-PE (UCHT1) (both from Becton
483 Dickinson, Franklin Lakes, NJ, USA) and CD8-Pacific Orange (3B5) (from Thermo Fisher
484 Scientific, Waltham, MA, USA). Cells were stained at room temperature for 20 min and sorted
485 with FACS Aria II (Becton Dickinson). Sytox blue (Thermo Fisher Scientific) was used to
486 exclude non-viable cells.

487

488 **Single peptides, matrix peptide pools and epitope mapping.** A set of 15-mers peptides with an
489 11-amino acid overlap spanning the 226 amino acids along the small S protein of hepatitis B
490 (HB) surface antigen (HBsAg), also designated as small HBs (SHBs) (Shouval, 2003), were
491 synthesized by JPT Peptide Technologies (Berlin, Germany). The set, composed of 54 **single**
492 **peptides** (See supplementary table 1), was used in a matrix-based strategy to map epitopes

493 against which the immune response is directed (Precopio et al., 2008). The matrix layout enables
494 efficient identification of epitopes within the antigen using a minimal number of cells. For this
495 purpose, a matrix of 15 pools, 7 rows and 8 columns, referred to as **matrix peptide pool**, was
496 designed so that each peptide is in exactly one row-pool and one column-pool, thereby allowing
497 for the identification of positive peptides at the intersection of positive pools. Matrix peptide
498 pools that induced a CD4 T cell response (as determined by CD40L/CD154 assay described
499 below) which meets the threshold criteria for a positive response were considered in the
500 deconvolution process. Top six single peptides were considered for peptide-specific T cell
501 expansion and sorting. A **master peptide pool** is composed of all of the 54 single peptides and
502 was used to identify and sort total vaccine-specific CD4 T cells. Each peptide was used at a final
503 concentration of 2 µg/ml.

504

505 ***Ex vivo* T cell stimulation (CD40L/CD154 assay).** Thawed PBMC from each vaccinee were
506 cultured in AIM-V medium that contained L-glutamine, streptomycin sulphate at 50 µg/ml, and
507 gentamicin sulphate at 10 µg/ml. (GIBCO, Grand Island, NY) and supplemented with 5% human
508 serum (One Lambda, Canoga Park, CA, USA). Cells were stimulated for 6 hours with 2 µg/ml of
509 each of the 15 matrix peptide pools in the presence of 1 µg/ml anti-CD40 antibody (HB14)
510 (purchased from Miltenyi Biotec, Bergisch Gladbach, Germany) and 1 µg/ml anti-CD28
511 antibody (CD28.2) (purchased from BD Biosciences, Franklin Lakes, NJ, USA).

512 Cells were stained using the following fluorochrome-labelled monoclonal antibodies: CD3-
513 PerCP (BW264/56), CD4-APC (REA623), CD8-VioGreen (REA734) and CD40L-PE (5C8)
514 (purchased from Miltenyi Biotec, Bergisch Gladbach, Germany). Viability dye Sytox blue from
515 Invitrogen (Thermo Fisher Scientific, Waltham, MA, USA) was used to exclude non-viable cells.

516 Data was acquired on FACS Aria II using Diva Software, both from BD Biosciences (Franklin
517 Lakes, NJ, USA), and analyzed on FlowJo software version 10.5.3 (Tree Star, Inc., Ashland, OR,
518 USA). Fluorescence-minus-one controls were performed in pilot studies. Gates for CD40L⁺CD4
519 T cells were set using cells left unstimulated.

520

521 ***In vitro* T cell expansion and cell sorting.** Thawed PBMC were labelled with
522 carboxyfluorescein succinimidyl ester (CFSE) (Invitrogen, Carlsbad, CA, USA) and cultured in
523 AIM-V medium that contained L-glutamine, streptomycin sulphate at 50 µg/ml, and gentamicin
524 sulphate at 10 µg/ml. (GIBCO, Grand Island, NY) and supplemented with 5% human serum
525 (One Lambda, Canoga Park, CA, USA). Cells were stimulated for 7 days with 2 µg/ml of
526 selected single peptides in addition to the master peptides pool. Cells were stained using the
527 following fluorochrome-labelled monoclonal antibodies: CD3-PerCP (BW264/56), CD4-APC
528 (REA623) and CD8-VioGreen (REA734) (purchased from Miltenyi Biotec, Bergisch Gladbach,
529 Germany). Viability dye Sytox blue from Invitrogen (Thermo Fisher Scientific, Waltham, MA,
530 USA) was used to exclude non-viable cells. Single viable CFSE^{low} CD3⁺ CD8⁻ CD4⁺ T cells
531 were sorted into 96-well PCR plates containing DNA/RNA Shield (Zymo Research, Irvine, CA,
532 USA) using FACS Aria II and Diva Software (BD Biosciences, Franklin Lakes, NJ, USA). For
533 each of the selected single peptides, 500 cells were sorted in two technical replicates. For the
534 master peptide pool, 1000 cells were sorted in two technical replicates. Plates were immediately
535 centrifuged and kept at – 20°C before TCR cDNA library preparation and sequencing.

536

537 **TCRβ cDNA Library Preparation and Sequencing of memory CD4 T cells.** DNA was
538 extracted from sorted memory CD4 T cells using Quick-DNA Microprep kit (Zymo Research,

539 Irvine, CA, USA). ImmunoSEQ hsTCRB sequencing kit (Adaptive Biotechnologies, Seattle,
540 WA, USA) was used to profile TCR β repertoire following the manufacturer's protocol.
541 After quality control using Fragment Analyzer (Agilent, Santa Clara, CA, USA), libraries were
542 pooled with equal volumes. The concentration of the final pool was measured with the Qubit™
543 dsDNA HS Assay kit (Thermo Fisher Scientific, Waltham, MA, USA). The final pool was
544 processed to be sequenced on the Miseq and NextSeq platforms (Illumina, San Diego, CA,
545 USA). Memory CD4 T cells of one of the vaccinees (H42, a non-converter) was not sequenced
546 due to a capacity issue.

547

548 **TCR cDNA Library Preparation and Sequencing of CFSE^{low} CD4 T cells.** RNA was
549 extracted from each of the two technical replicates of sorted CFSE^{low} CD4 T cells using Quick-
550 RNA Microprep kit (Zymo Research, Irvine, CA, USA). Without measuring the resulted RNA
551 concentration, an RNA-based library preparation was used. The QIAseq Immune Repertoire
552 RNA Library kit (Qiagen, Venlo, Netherlands) amplifies TCR alpha, beta, gamma and delta
553 chains. After quality control using Fragment Analyzer (Agilent, Santa Clara, CA, USA),
554 concentration was measured with the Qubit™ dsDNA HS Assay kit (Thermo Fisher Scientific,
555 Waltham, MA, USA) and pools were equimolarly pooled and prepared for sequencing on the
556 Nextseq platform (Illumina, San Diego, CA, USA).

557

558 **TCR β Sequence Analysis.** TCR β clonotypes were identified as previously described (de Neuter
559 et al., 2018) where a unique TCR β clonotype is defined as a unique combination of a V gene,
560 CDR3 amino acid sequence, and J gene. All memory CD4 T cell DNA-based TCR β sequencing
561 reads were annotated using the immunoSEQ analyzer (v2) from Adaptive Biotechnologies. All

562 small bulk RNA-based TCR sequencing reads were annotated using the MiXCR tool (v3.0.7)
563 from the FASTQ files. As all RNA-based TCR sequencing experiments featured two technical
564 replicates, only those TCR sequences that occurred in both replicates were retained and their
565 counts were summed. Tracking of vaccine-specific TCR β clonotypes is based on exact TCR β
566 CDR3 amino acid matches to remove any bias introduced by the different VDJ annotation
567 pipelines. Non-HBsAg TCR annotations were done with the TCRex web tool (Gielis et al., 2019)
568 on the 24th of July, 2019 using version 0.3.0. Inference of similar epitope binding between two
569 TCR sequences is defined according to the Hamming distance (d) calculated on the CDR3 amino
570 acid sequence with a cutoff c , as supported by Meysman et al. (Meysman et al., 2018). All scripts
571 used in this analysis are available via github (<https://github.com/pmeysman/HepBTCR>).

572

573 **Predictive HBs-response model.** From the single peptide data generated in the matrix peptide
574 pool experiments, we aimed to create a predictive model to enumerate the HBs response from
575 full TCR β repertoire data. This approach allows for predictions that are epitope-specific rather
576 than simply vaccine-specific. This model was applied in a leave-one-out cross validation so that
577 vaccine-specific TCR β sequences from a vaccinee are not used to make predictions for the same
578 vaccinee. While the predictive model is derived from epitope-specific data, it cannot be
579 guaranteed that some of the expanded CD4 T cells detected in the in vitro assay are not due to
580 bystander activation. Vaccine-specific TCR β sequences of vaccinees who did not respond to the
581 vaccine at day 60 (late-converters and non-converters) are expected to be more enriched in cells
582 triggered to expand due to bystander activation. Indeed, running the set of vaccine-specific
583 TCR β sequences through the TCRex webtool (Gielis et al., 2019) reveals that several TCRs are
584 predicted to be highly similar to those reactive to the CMV NLVPMVATV epitope (enrichment

585 P value <0.001 when compared to the TCReX background repertoire) and the Mart-1 variant
586 ELAGIGILTV epitope (P value <0.001), which supports the notion that some of these TCR β
587 sequences might not be specific to HBsAg. This set of vaccine-specific TCR β sequences can
588 thus be used to make predictions about possible TCR β sequences due to bystander activation of
589 CD4 T cells, i.e. common TCR β sequences that might be present as false positives. The final
590 output of the model is thus a ratio, R_{hbs} , for any repertoire rep_i describing a set of TCR β
591 sequences t_{rep_i} :

$$R_{hbs}(t_{rep_i}) = \frac{\sum_{pep=1}^{54} |\{t_{rep_i} | d(t_{rep_i}, t_{pep}) < c\}| / |t_{pep}|}{|\{t_{rep_i} | d(t_{rep_i}, t_{bystander}) < c\}| / |t_{bystander}|}$$

592 with t_{pep} as the set of TCR β sequences occurring in both biological replicates for a single sample
593 and a single peptide (pep) from the HBsAg matrix peptide pool experiment, and $t_{bystander}$ as the
594 set of TCR β sequences occurring in both biological replicates of the master peptide pool in any
595 of the non-responding samples. Thus the ratio signifies the number of TCR clonotypes predicted
596 to be reactive against one of the HBsAg peptides, normalized by a count of putative false
597 positive predictions from bystander T-cells.

598

599 ***Ex vivo* T cell phenotyping of vaccine-specific T cells.** Thawed PBMC from each vaccinee
600 were cultured in AIM-V medium that contained L-glutamine, streptomycin sulphate at 50 μ g/ml,
601 and gentamicin sulphate at 10 μ g/ml. (GIBCO, Grand Island, NY) and supplemented with 5%
602 human serum (One Lambda, Canoga Park, CA, USA). Cells were stimulated for 6 hours with 2
603 μ g/ml of a master peptide pool representing the full length of the small surface envelope protein
604 of hepatitis B, in the presence of 1 μ g/ml anti-CD40 antibody (HB14) (purchased from Miltenyi
605 Biotec, Bergisch Gladbach, Germany) and 1 μ g/ml anti-CD28 antibody (CD28.2) (purchased

606 from BD Biosciences, Franklin Lakes, NJ, USA). Cells were stained using the following
607 fluorochrome-labelled monoclonal antibodies:
608 CD3-BV510 (SK7), CD4-PerCP/Cy5.5 (RPA-T4), CD8-APC/Cy7 (SK1), CD45RA-AF488
609 (HI100), CD25-BV421 (M-A251), CD127-BV785 (A019D5) and CD137-PE (4-1BB)
610 (purchased from BioLegend, San Diego, CA, USA), CXCR5 (CD185)-PE-eFluor 610
611 (MU5UBEE) (from eBioscience, Thermo Fisher Scientific, Waltham, MA, USA) and CD40L-
612 APC (5C8) (purchased from Miltenyi Biotec, Bergisch Gladbach, Germany). Fixable viability
613 dye Zombie NIR™ from BioLegend (San Diego, CA, USA) was used to exclude non-viable
614 cells. Data was acquired on FACS Aria II using Diva Software, both from BD Biosciences
615 (Franklin Lakes, NJ, USA), and analyzed on FlowJo software version 10.5.3 (Tree Star, Inc.,
616 Ashland, OR, USA) using gating strategy shown in **Fig. S1a**. Fluorescence-minus-one controls
617 were performed in pilot studies. Gates for CD40L⁺ and 4-1BB⁺ CD4 T cells (**Fig. S1b**) were set
618 using cells left unstimulated (negative control contained DMSO at the same concentration used
619 to solve peptide pools). In order to account for background expression of CD40L and 4-1BB on
620 CD4 T cells, responses in cells left unstimulated were subtracted from the responses to peptides,
621 and when peptides-specific CD40L⁺ or 4-1BB⁺ CD4 T cells were not significantly higher than
622 those detected for cells left unstimulated (using one-sided Fisher's exact test), values were
623 mutated to zero.

624

625 **Statistics and data visualization.** The two-sided Fisher's exact test was used to evaluate the
626 significance of relationship between early/late-converters and CMV, EBV or HSV seropositivity.
627 For the visualization of marker expression, TCR β counts and cell frequencies between time
628 points or groups of vaccinees, ggplot2 (V3.3.2) and ggpubr (V0.2.5) packages in R were used.

629 The Wilcoxon signed-rank test was used to compare two or more groups, with unpaired and
630 paired analysis as necessary. The nonparametric Spearman's rank-order correlation was used to
631 test for correlation. We used the following convention for symbols indicating statistical
632 significance; ns $P > 0.05$, * $P \leq 0.05$, ** $P \leq 0.01$, *** $P \leq 0.001$, **** $P \leq 0.0001$.

633

634 **Study approval.** Protocols involving the use of human tissues were approved by the Ethics
635 Committee of Antwerp University Hospital and University of Antwerp (Antwerp, Belgium), and
636 all of the experiments were performed in accordance with the protocols.

637

638 **Data availability**

639 The sequencing data that support the findings of this study have been deposited on Zenodo
640 (<https://doi.org/10.5281/zenodo.3989144>). Flow Cytometry Standard (FCS) data files with
641 associated FlowJo workspaces are deposited at flowrepository.org (Spidlen et al., 2012) under
642 the following experiment names: epitope mapping: <https://flowrepository.org/id/FR-FCM-Z2TN>;
643 *in vitro* T cell expansion: <https://flowrepository.org/id/FR-FCM-Z2TM>; *ex vivo* CD4 T cell
644 assay: <https://flowrepository.org/id/FR-FCM-Z2TL>.

645

646

647

648

649 **References**

- 650 Bacher, P., Schink, C., Teutschbein, J., Kniemeyer, O., Assenmacher, M., Brakhage, A.A., and Scheffold, A. (2013). Antigen-reactive T cell
651 enrichment for direct, high-resolution analysis of the human naive and memory Th cell repertoire. *J. Immunol.* *190*, 3967–3976.
- 652 Bacher, P., Kniemeyer, O., Teutschbein, J., Thön, M., Vödisch, M., Wartenberg, D., Scharf, D.H., Koester-Eiserfunke, N., Schütte, M., Dübel, S.,
653 et al. (2014a). Identification of Immunogenic Antigens from *Aspergillus fumigatus* by Direct Multiparameter Characterization of Specific
654 Conventional and Regulatory CD4⁺ T Cells. *J. Immunol.* *193*, 3332–3343.
- 655 Bacher, P., Kniemeyer, O., Schönbrunn, A., Sawitzki, B., Assenmacher, M., Rietschel, E., Steinbach, A., Cornely, O.A., Brakhage, A.A., Thiel,
656 A., et al. (2014b). Antigen-specific expansion of human regulatory T cells as a major tolerance mechanism against mucosal fungi. *Mucosal*
657 *Immunol.* *7*, 916–928.
- 658 Becattini, S., Latorre, D., Mele, F., Foglierini, M., De Gregorio, C., Cassotta, A., Fernandez, B., Kelderman, S., Schumacher, T.N., Corti, D., et
659 al. (2015). Functional heterogeneity of human memory CD4⁺ T cell clones primed by pathogens or vaccines. *Science* (80-.). *347*, 400–406.
- 660 Bentebibel, S.-E., Schmitt, N., Banchereau, J., and Ueno, H. (2011). Human tonsil B-cell lymphoma 6 (BCL6)-expressing CD4⁺ T-cell subset
661 specialized for B-cell help outside germinal centers. *Proc. Natl. Acad. Sci.* *108*, E488–E497.
- 662 Blom, K., Braun, M., Ivarsson, M.A., Gonzalez, V.D., Falconer, K., Moll, M., Ljunggren, H.-G., Michaëlsson, J., and Sandberg, J.K. (2013).
663 Temporal Dynamics of the Primary Human T Cell Response to Yellow Fever Virus 17D As It Matures from an Effector- to a Memory-Type
664 Response. *J. Immunol.* *190*, 2150–2158.
- 665 Booth, N.J., McQuaid, A.J., Sobande, T., Kissane, S., Agius, E., Jackson, S.E., Salmon, M., Falciani, F., Yong, K., Rustin, M.H., et al. (2010).
666 Different Proliferative Potential and Migratory Characteristics of Human CD4⁺ Regulatory T Cells That Express either CD45RA or CD45RO. *J.*
667 *Immunol.* *184*, 4317–4326.
- 668 Brezar, V., Godot, V., Cheng, L., Su, L., Lévy, Y., and Seddiki, N. (2016). T-regulatory cells and vaccination “pay attention and do not neglect
669 them”: Lessons from HIV and cancer vaccine trials. *Vaccines* *4*.
- 670 Campion, S.L., Brodie, T.M., Fischer, W., Korber, B.T., Rossetti, A., Goonetilleke, N., McMichael, A.J., and Sallusto, F. (2014). Proteome-wide
671 analysis of HIV-specific naive and memory CD4⁺ T cells in unexposed blood donors. *J. Exp. Med.* *211*, 1273–1280.
- 672 Chou, H.H., Chien, W.H., Wu, L.L., Cheng, C.H., Chung, C.H., Horng, J.H., Ni, Y.H., Tseng, H.T., Wu, D., Lu, X., et al. (2015). Age-related
673 immune clearance of hepatitis B virus infection requires the establishment of gut microbiota. *Proc. Natl. Acad. Sci. U. S. A.* *112*, 2175–2180.
- 674 Curtsinger, J.M., and Mescher, M.F. (2010). Inflammatory cytokines as a third signal for T cell activation. *Curr. Opin. Immunol.* *22*, 333–340.
- 675 DeWitt, W.S., Emerson, R.O., Lindau, P., Vignali, M., Snyder, T.M., Desmarais, C., Sanders, C., Utsugi, H., Warren, E.H., McElrath, J., et al.
676 (2015). Dynamics of the Cytotoxic T Cell Response to a Model of Acute Viral Infection. *J. Virol.* *89*, 4517–4526.
- 677 DeWitt, W.S., Smith, A., Schoch, G., Hansen, J.A., Matsen, F.A., and Bradley, P. (2018). Human T cell receptor occurrence patterns encode
678 immune history, genetic background, and receptor specificity. *Elife* *7*.
- 679 Elias, G., Ogunjimi, B., and Van Tendeloo, V. (2020). Activation-induced surface proteins in the identification of antigen-responsive CD4 T
680 cells. *Immunol. Lett.* *219*, 1–7.
- 681 Emerson, R.O., DeWitt, W.S., Vignali, M., Gravley, J., Hu, J.K., Osborne, E.J., Desmarais, C., Klinger, M., Carlson, C.S., Hansen, J.A., et al.
682 (2017). Immunosequencing identifies signatures of cytomegalovirus exposure history and HLA-mediated effects on the T cell repertoire. *Nat.*

- 683 Genet. 49, 659–665.
- 684 Esensten, J.H., Helou, Y.A., Chopra, G., Weiss, A., and Bluestone, J.A. (2016). CD28 Costimulation: From Mechanism to Therapy. *Immunity*
- 685 44, 973–988.
- 686 Farber, D.L., Yudanin, N.A., and Restifo, N.P. (2014). Human memory T cells: Generation, compartmentalization and homeostasis. *Nat. Rev.*
- 687 *Immunol.* 14, 24–35.
- 688 Fonseca, V.R., Agua-Doce, A., Maceiras, A.R., Pierson, W., Ribeiro, F., Romão, V.C., Pires, A.R., Silva, S.L. da, Fonseca, J.E., Sousa, A.E., et
- 689 al. (2017). Human blood Tfr cells are indicators of ongoing humoral activity not fully licensed with suppressive function. *Sci. Immunol.* 2.
- 690 Frentsch, M., Arbach, O., Kirchoff, D., Moewes, B., Worm, M., Rothe, M., Scheffold, A., and Thiel, A. (2005). Direct access to CD4+ T cells
- 691 specific for defined antigens according to CD154 expression. *Nat. Med.* 11, 1118–1124.
- 692 Furman, D., Jojic, V., Sharma, S., Shen-Orr, S.S., Angel, C.J.L., Onengut-Gumuscu, S., Kidd, B.A., Maecker, H.T., Concannon, P., Dekker, C.L.,
- 693 et al. (2015). Cytomegalovirus infection enhances the immune response to influenza. *Sci. Transl. Med.* 7, 281ra43.
- 694 Galson, J.D., Trück, J., Clutterbuck, E.A., Fowler, A., Cerundolo, V., Pollard, A.J., Lunter, G., and Kelly, D.F. (2016). B-cell repertoire dynamics
- 695 after sequential hepatitis B vaccination and evidence for cross-reactive B-cell activation. *Genome Med.* 8, 68.
- 696 Garner-Spitzer, E., Wagner, A., Paulke-Korinek, M., Kollaritsch, H., Heinz, F.X., Redlberger-Fritz, M., Stiasny, K., Fischer, G.F., Kundi, M.,
- 697 and Wiedermann, U. (2013). Tick-Borne Encephalitis (TBE) and Hepatitis B Nonresponders Feature Different Immunologic Mechanisms in
- 698 Response to TBE and Influenza Vaccination with Involvement of Regulatory T and B Cells and IL-10. *J. Immunol.* 191, 2426–2436.
- 699 Gielis, S., Moris, P., Bittremieux, W., De Neuter, N., Ogunjimi, B., Laukens, K., and Meysman, P. (2019). Detection of Enriched T Cell Epitope
- 700 Specificity in Full T Cell Receptor Sequence Repertoires. *Front. Immunol.* 10.
- 701 Ito, T., Hanabuchi, S., Wang, Y.H., Park, W.R., Arima, K., Bover, L., Qin, F.X.F., Gilliet, M., and Liu, Y.J. (2008). Two Functional Subsets of
- 702 FOXP3+ Regulatory T Cells in Human Thymus and Periphery. *Immunity* 28, 870–880.
- 703 Kachapati, K., Adams, D.E., Wu, Y., Steward, C.A., Rainbow, D.B., Wicker, L.S., Mittler, R.S., and Ridgway, W.M. (2012). The B10 Idd9.3
- 704 locus mediates accumulation of functionally superior CD137(+) regulatory T cells in the nonobese diabetic type 1 diabetes model. *J. Immunol.*
- 705 189, 5001–5015.
- 706 Keating, G.M., and Noble, S. (2003). Recombinant Hepatitis B Vaccine (Engerix-B). *Drugs* 63, 1021–1051.
- 707 Kim, Y.H., Choi, B.K., Shin, S.M., Kim, C.H., Oh, H.S., Park, S.H., Lee, D.G., Lee, M.J., Kim, K.H., Vinay, D.S., et al. (2011). 4-1BB
- 708 Triggering Ameliorates Experimental Autoimmune Encephalomyelitis by Modulating the Balance between Th17 and Regulatory T Cells. *J.*
- 709 *Immunol.* 187, 1120–1128.
- 710 Klarenbeek, P.L., Tak, P.P., van Schaik, B.D.C., Zwinderman, A.H., Jakobs, M.E., Zhang, Z., van Kampen, A.H.C., van Lier, R.A.W., Baas, F.,
- 711 and de Vries, N. (2010). Human T-cell memory consists mainly of unexpanded clones. *Immunol. Lett.* 133, 42–48.
- 712 Kohler, S., Bethke, N., Böthe, M., Sommerick, S., Frentsch, M., Romagnani, C., Niedrig, M., and Thiel, A. (2012). The early cellular signatures
- 713 of protective immunity induced by live viral vaccination. *Eur. J. Immunol.* 42, 2363–2373.
- 714 Krangel, M.S. (2009). Mechanics of T cell receptor gene rearrangement. *Curr. Opin. Immunol.* 21, 133–139.
- 715 Lanteri, M.C., O'Brien, K.M., Purtha, W.E., Cameron, M.J., Lund, J.M., Owen, R.E., Heitman, J.W., Custer, B., Hirschhorn, D.F., Tobler, L.H.,
- 716 et al. (2009). Tregs control the development of symptomatic West Nile virus infection in humans and mice. *J. Clin. Invest.* 119, 3266–3277.
- 717 Lin, P.H., Wong, W.I., Wang, Y.L., Hsieh, M.P., Lu, C.W., Liang, C.Y., Jui, S.H., Wu, F.Y., Chen, P.J., and Yang, H.C. (2018). Vaccine-induced

- 718 antigen-specific regulatory T cells attenuate the antiviral immunity against acute influenza virus infection. *Mucosal Immunol.* *11*, 1239–1253.
- 719 Liu, W., Putnam, A.L., Xu-yu, Z., Szot, G.L., Lee, M.R., Zhu, S., Gottlieb, P.A., Kapranov, P., Gingeras, T.R., Barbara, B.F., et al. (2006).
- 720 CD127 expression inversely correlates with FoxP3 and suppressive function of human CD4+ T reg cells. *J. Exp. Med.* *203*, 1701–1711.
- 721 Lovelace, P., and Maecker, H.T. (2018). Multiparameter Intracellular Cytokine Staining. In *Methods in Molecular Biology* (Clifton, N.J.), pp.
- 722 151–166.
- 723 Mason, G.M., Lowe, K., Melchiotti, R., Ellis, R., de Rinaldis, E., Peakman, M., Heck, S., Lombardi, G., and Tree, T.I.M. (2015). Phenotypic
- 724 Complexity of the Human Regulatory T Cell Compartment Revealed by Mass Cytometry. *J. Immunol.* *195*, 2030–2037.
- 725 McHugh, R.S., Whitters, M.J., Piccirillo, C.A., Young, D.A., Shevach, E.M., Collins, M., and Byrne, M.C. (2002). CD4(+)CD25(+)
- 726 immunoregulatory T cells: gene expression analysis reveals a functional role for the glucocorticoid-induced TNF receptor. *Immunity* *16*, 311–
- 727 323.
- 728 Meireles, L.C., Marinho, R.T., and Van Damme, P. (2015). Three decades of hepatitis B control with vaccination. *World J. Hepatol.* *7*, 2127–
- 729 2132.
- 730 Meysman, P., De Neuter, N., Gielis, S., Bui Thi, D., Ogunjimi, B., and Laukens, K. (2018). On the viability of unsupervised T-cell receptor
- 731 sequence clustering for epitope preference. *Bioinformatics* *35*, 1461–1468.
- 732 Mittler, R.S., Bailey, T.S., Klussman, K., Trailsmith, M.D., and Hoffmann, M.K. (1999). Anti-4-1BB monoclonal antibodies abrogate T cell-
- 733 dependent humoral immune responses in vivo through the induction of helper T cell anergy. *J. Exp. Med.* *190*, 1535–1540.
- 734 Miyara, M., Yoshioka, Y., Kitoh, A., Shima, T., Wing, K., Niwa, A., Parizot, C., Taflin, C., Heike, T., Valeyre, D., et al. (2009). Functional
- 735 Delineation and Differentiation Dynamics of Human CD4+ T Cells Expressing the FoxP3 Transcription Factor. *Immunity* *30*, 899–911.
- 736 Mohr, A., Malhotra, R., Mayer, G., Gorochov, G., and Miyara, M. (2018). Human FOXP3+ T regulatory cell heterogeneity. *Clin. Transl.*
- 737 *Immunol.* *7*.
- 738 de Neuter, N., Bartholomeus, E., Elias, G., Keersmaekers, N., Suls, A., Jansens, H., Smits, E., Hens, N., Beutels, P., van Damme, P., et al. (2018).
- 739 Memory CD4+T cell receptor repertoire data mining as a tool for identifying cytomegalovirus serostatus. *Genes Immun.*
- 740 De Neuter, N., Bittremieux, W., Beirnaert, C., Cuypers, B., Mrzic, A., Moris, P., Suls, A., Van Tendeloo, V., Ogunjimi, B., Laukens, K., et al.
- 741 (2018). On the feasibility of mining CD8+ T cell receptor patterns underlying immunogenic peptide recognition. *Immunogenetics* *70*, 159–168.
- 742 Pogorelyy, M. V., Minervina, A.A., Touzel, M.P., Sycheva, A.L., Komech, E.A., Kovalenko, E.I., Karganova, G.G., Egorov, E.S., Komkov,
- 743 A.Y., Chudakov, D.M., et al. (2018). Precise tracking of vaccine-responding T cell clones reveals convergent and personalized response in
- 744 identical twins. *Proc. Natl. Acad. Sci. U. S. A.* *115*, 12704–12709.
- 745 Precopio, M.L., Butterfield, T.R., Casazza, J.P., Little, S.J., Richman, D.D., Koup, R.A., and Roederer, M. (2008). Optimizing peptide matrices
- 746 for identifying T-cell antigens. *Cytom. Part A* *73*, 1071–1078.
- 747 Reece, W.H.H., Pinder, M., Gothard, P.K., Milligan, P., Bojang, K., Doherty, T., Plebanski, M., Akinwunmi, P., Everaere, S., Watkins, K.R., et
- 748 al. (2004). A CD4+ T-cell immune response to a conserved epitope in the circumsporozoite protein correlates with protection from natural
- 749 *Plasmodium falciparum* infection and disease. *Nat. Med.* *10*, 406–410.
- 750 Reese, T.A., Bi, K., Kambal, A., Filali-Mouhim, A., Beura, L.K., Bürger, M.C., Pulendran, B., Sekaly, R.P., Jameson, S.C., Masopust, D., et al.
- 751 (2016). Sequential Infection with Common Pathogens Promotes Human-like Immune Gene Expression and Altered Vaccine Response. *Cell Host*
- 752 *Microbe* *19*, 713–719.

- 753 Ritchie, A.J., Campion, S.L., Kopycinski, J., Moodie, Z., Wang, Z.M., Pandya, K., Moore, S., Liu, M.K.P., Brackenridge, S., Kuldane, K., et al.
754 (2011). Differences in HIV-Specific T Cell Responses between HIV-Exposed and -Unexposed HIV-Seronegative Individuals. *J. Virol.* *85*, 3507–
755 3516.
- 756 Robinson, C.M., and Pfeiffer, J.K. (2014). Viruses and the Microbiota. *Annu. Rev. Virol.* *1*, 55–69.
- 757 Rudensky, A.Y. (2011). Regulatory T cells and Foxp3. *Immunol. Rev.* *241*, 260–268.
- 758 Rudolph, M.G., Stanfield, R.L., and Wilson, I.A. (2006). HOW TCRS BIND MHCS, PEPTIDES, AND CORECEPTORS. *Annu. Rev. Immunol.*
759 *24*, 419–466.
- 760 Sallusto, F., Lanzavecchia, A., Araki, K., and Ahmed, R. (2010). From vaccines to memory and back. *Immunity* *33*, 451–463.
- 761 Sanchez, A.M., Zhu, J., Huang, X., and Yang, Y. (2012). The Development and Function of Memory Regulatory T Cells after Acute Viral
762 Infections. *J. Immunol.* *189*, 2805–2814.
- 763 Schoenbrunn, A., Frensch, M., Kohler, S., Keye, J., Dooms, H., Moewes, B., Dong, J., Loddenkemper, C., Sieper, J., Wu, P., et al. (2012). A
764 converse 4-1BB and CD40 ligand expression pattern delineates activated regulatory T cells (Treg) and conventional T cells enabling direct
765 isolation of alloantigen-reactive natural Foxp3+ Treg. *J. Immunol.* *189*, 5985–5994.
- 766 Seddiki, N., Santner-Nanan, B., Martinson, J., Zaunders, J., Sasson, S., Landay, A., Solomon, M., Selby, W., Alexander, S.I., Nanan, R., et al.
767 (2006). Expression of interleukin (IL)-2 and IL-7 receptors discriminates between human regulatory and activated T cells. *J. Exp. Med.* *203*,
768 1693–1700.
- 769 Sewell, A.K. (2012). Why must T cells be cross-reactive? *Nat. Rev. Immunol.* *12*, 669–677.
- 770 Shouval, D. (2003). Hepatitis B vaccines. *J. Hepatol.* *39*, 70–76.
- 771 Spidlen, J., Breuer, K., Rosenberg, C., Kotecha, N., and Brinkman, R.R. (2012). FlowRepository: A resource of annotated flow cytometry
772 datasets associated with peer-reviewed publications. *Cytom. Part A* *81 A*, 727–731.
- 773 Su, L.F., and Davis, M.M. (2013). Antiviral memory phenotype T cells in unexposed adults. *Immunol. Rev.* *255*, 95–109.
- 774 Su, L.F., Kidd, B.A., Han, A., Kotzin, J.J., and Davis, M.M. (2013). Virus-Specific CD4+ Memory-Phenotype T Cells Are Abundant in
775 Unexposed Adults. *Immunity* *38*, 373–383.
- 776 Turner, S.J., La Gruta, N.L., Kedzierska, K., Thomas, P.G., and Doherty, P.C. (2009). Functional implications of T cell receptor diversity. *Curr.*
777 *Opin. Immunol.* *21*, 286–290.
- 778 Wilson, D.B., Wilson, D.H., Schroder, K., Pinilla, C., Blondelle, S., Houghten, R.A., and Garcia, K.C. (2004). Specificity and degeneracy of T
779 cells. *Mol. Immunol.* *40*, 1047–1055.
- 780 Wing, J.B., Ise, W., Kurosaki, T., and Sakaguchi, S. (2014). Regulatory T cells control antigen-specific expansion of Tfh cell number and
781 humoral immune responses via the coreceptor CTLA-4. *Immunity* *41*, 1013–1025.
- 782 Winkler, E.S., and Thackray, L.B. (2019). A long-distance relationship: the commensal gut microbiota and systemic viruses. *Curr. Opin. Virol.*
783 *37*, 44–51.
- 784 Wu, T., Li, F., Chen, Y., Wei, H., Tian, Z., Sun, C., and Sun, R. (2019). CD4+ T cells play a critical role in microbiota-maintained Anti-HBV
785 immunity in a mouse model. *Front. Immunol.* *10*.
- 786 Yuen, M.-F., Chen, D.-S., Dusheiko, G.M., Janssen, H.L.A., Lau, D.T.Y., Locarnini, S.A., Peters, M.G., and Lai, C.-L. (2018). Hepatitis B virus
787 infection. *Nat. Rev. Dis. Prim.* *4*, 18035.

788 Zheng, G., Wang, B., and Chen, A. (2004). The 4-1BB costimulation augments the proliferation of CD4+CD25+ regulatory T cells. *J. Immunol.*

789 *173*, 2428–2434.

790

791

792

793

794

795

796

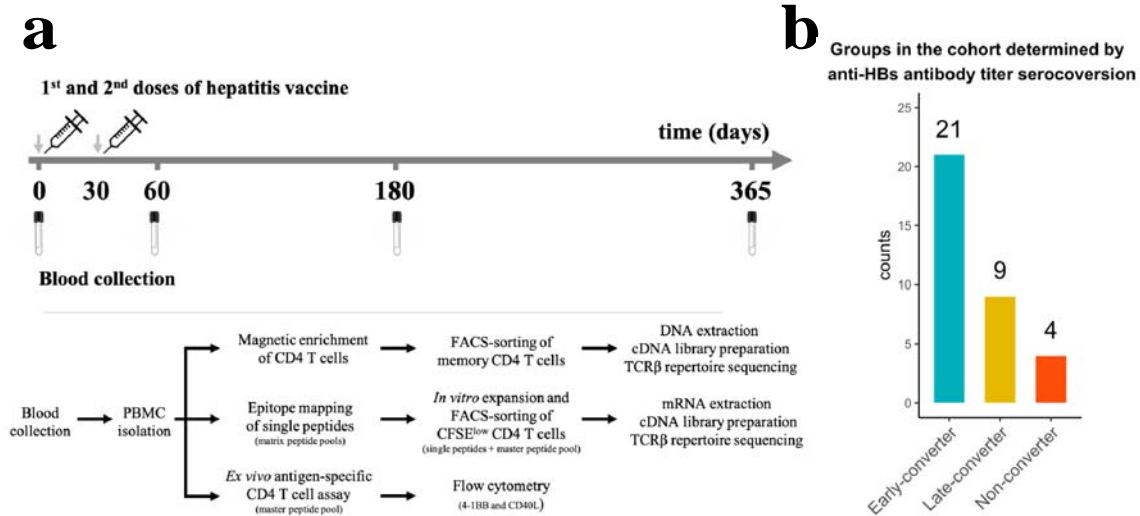
797

798

799

800

801



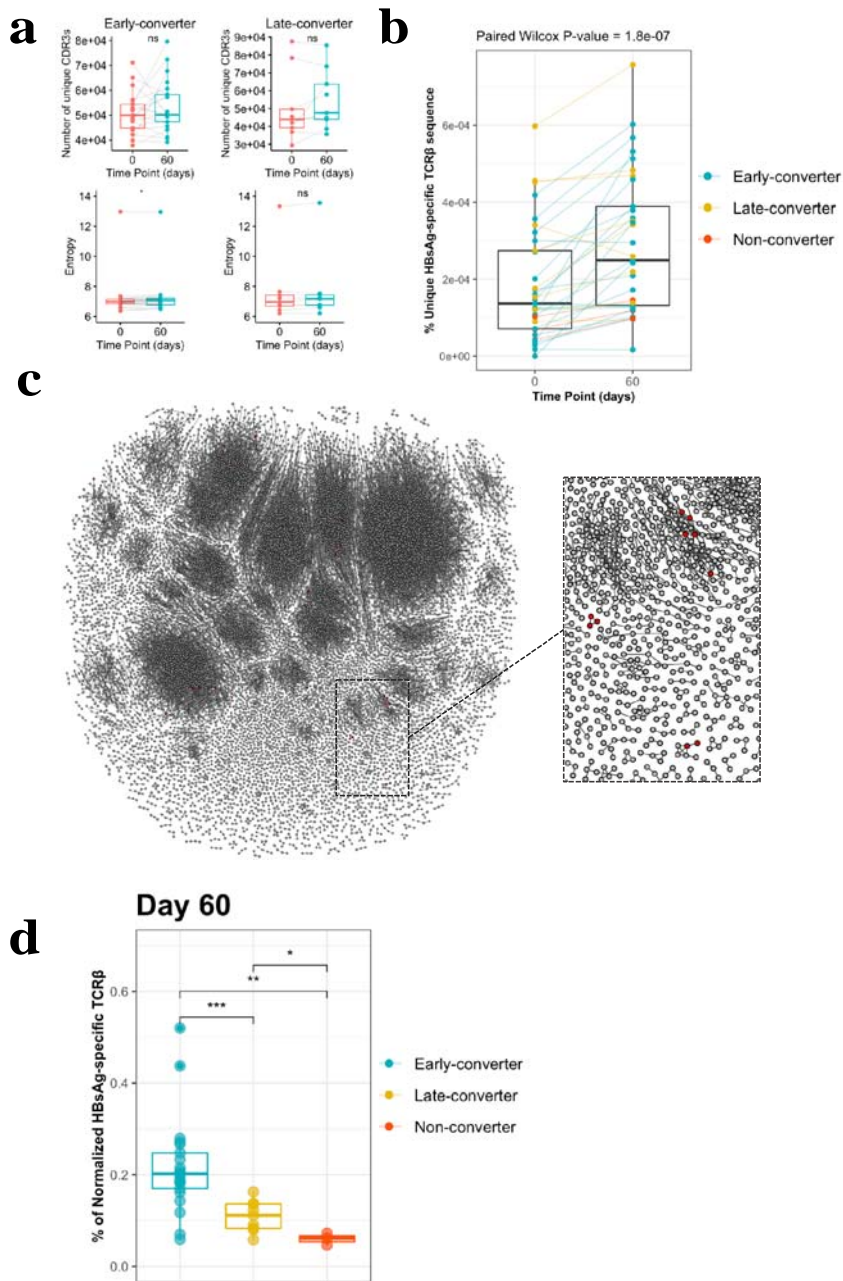
802

Figure 1. Hepatitis B vaccination (Engerix-B®) study design.

803 **a** Hepatitis B (Engerix-B®) vaccination and experimental design. (Top) Timeline of vaccination and blood
804 collection. (Bottom) Memory CD4 T cells were magnetically enriched and FACS-sorted from two time points (day
805 0 and day 60) for TCRβ repertoire sequencing. Matrix peptide pools were used to map CD4 T cell epitopes of the
806 vaccine from PBMCs collected at day 60 and to select single peptides. After 7 days of *in vitro* expansion, single
807 peptide-specific and master peptide pool-specific CFSE^{low} CD4 T cells from PBMCs collected at day 60 were
808 FACS-sorted in two technical replicates for TCRβ repertoire sequencing. PBMCs collected at days 0, 60, 180, and
809 365 were stimulated with the master peptide pool (HBsAg) and assessed for converse expression of 4-1BB and
810 CD40L by flow cytometry.

811 **b** Vaccinee cohort can be classified into three groups as determined by anti-Hepatitis B surface (anti-HBs) titer over
812 four time points.

813 Early-converters seroconverted at day 60, late-converters seroconverted at day 180 or day 365 and non-converters
814 did not have an anti-HBs titer higher than 10 IU/ml at any of the time points.
815



816

817 **Figure 2. CD4 T cell memory TCR β repertoire and vaccine-specific TCR β clonotypes.**

818 a Comparison of the memory CD4 TCR β repertoire diversity and entropy between day 0 and day

819 60.

820 b Frequency of unique vaccine-specific TCR β sequences out of total sequenced TCR β sequences

821 between two time points for all vaccinees colored by group.

822 c Sequenced CD4⁺ TCR memory repertoire of vaccinee H35 at day 60. Each TCR clonotype is

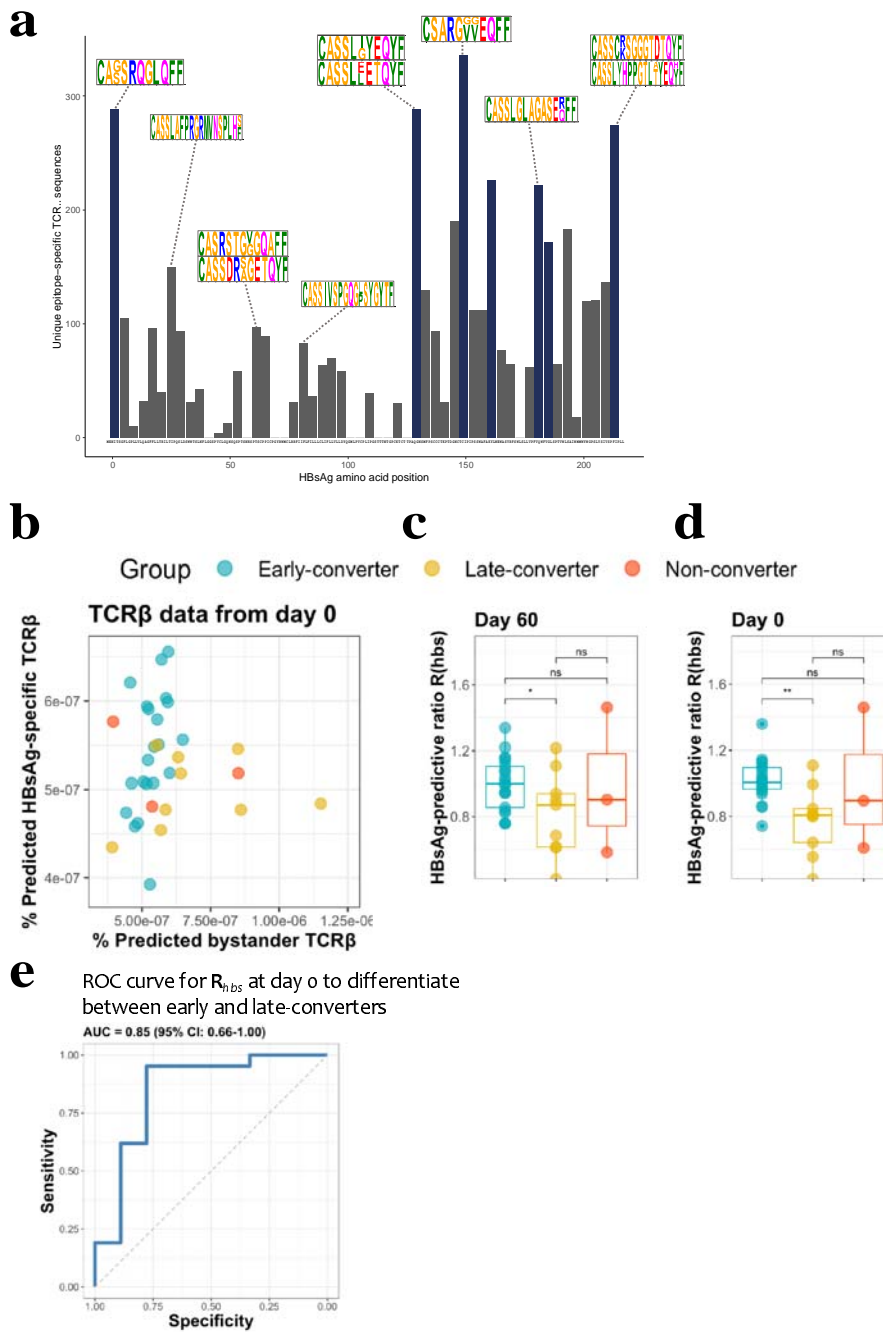
823 represented by a node. TCRs are connected by an edge if their Hamming distance is one. Only

824 clusters with at least three TCRs are shown. TCR clonotypes in red are the vaccine-specific

825 TCR β sequences that were not present prior to vaccination.

826 d Frequency of vaccine-specific TCR β sequences within memory CD4 T cell repertoire
827 normalized by number of HBsAg-specific TCR β sequences found for each vaccinee at time point
828 60.
829

830



831

832

Figure 3. HBsAg peptide-specific TCR β identification and predictive potential of R_{hbs} .

833

a Overview of the detected HBsAg epitope-specific TCR β sequences. Each bar corresponds to unique TCR β

834

sequences found against a single 15mer HBsAg peptide, with 11 amino acid overlap to each subsequent peptide.

835

Bars in blue denote those epitopes for which 10 or more volunteers had a strong T-cell reaction. Motif logos on top

836

of bars denote a sampling of the most common TCR β amino acid sequence motifs for those epitopes.

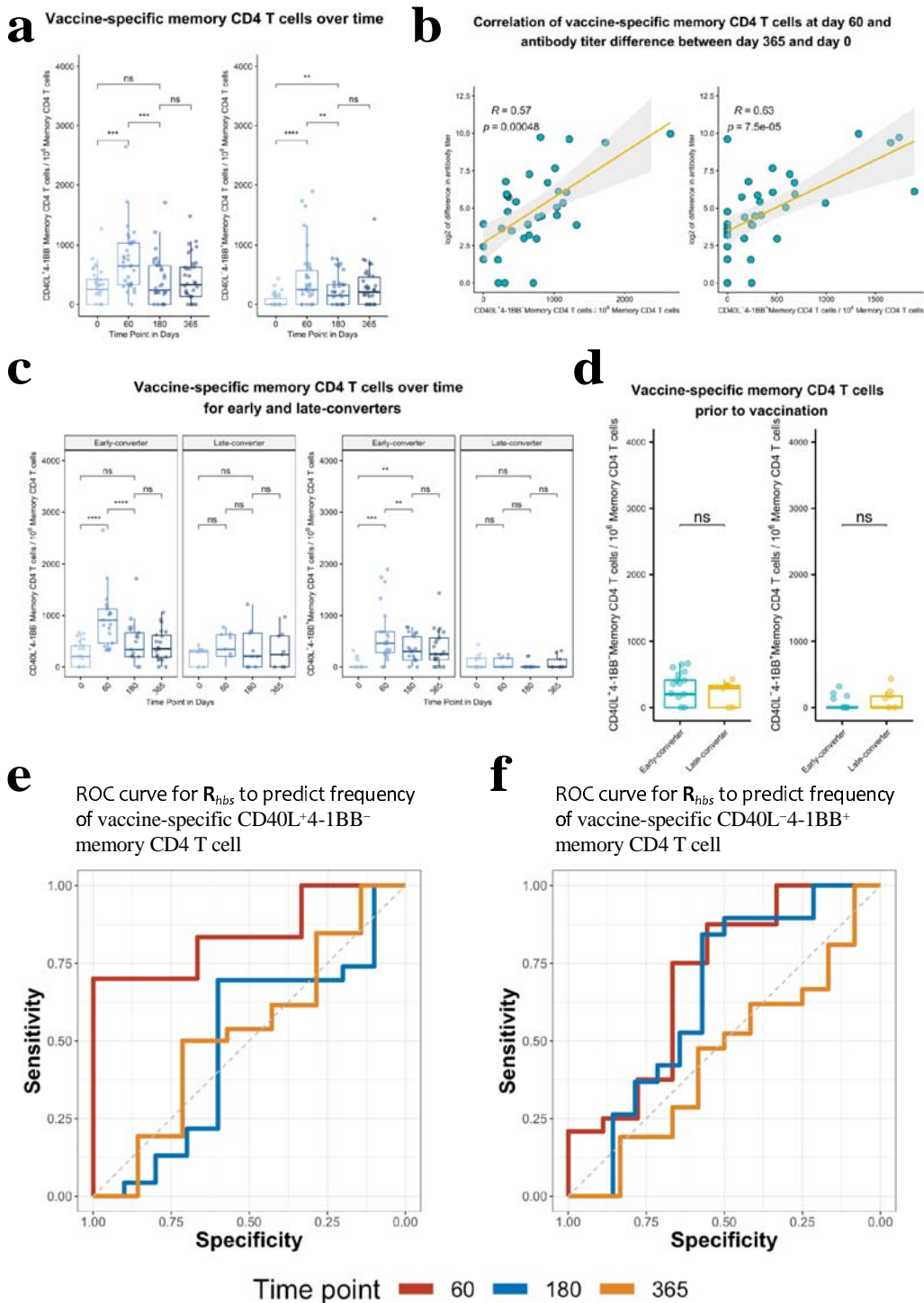
837

b Scatter plot with the frequency of predicted HBsAg epitope-specific and bystander TCR β sequences. Predictions

838

done as a leave-one-out cross-validation. Each circle represents a vaccinee with the color denoting the response

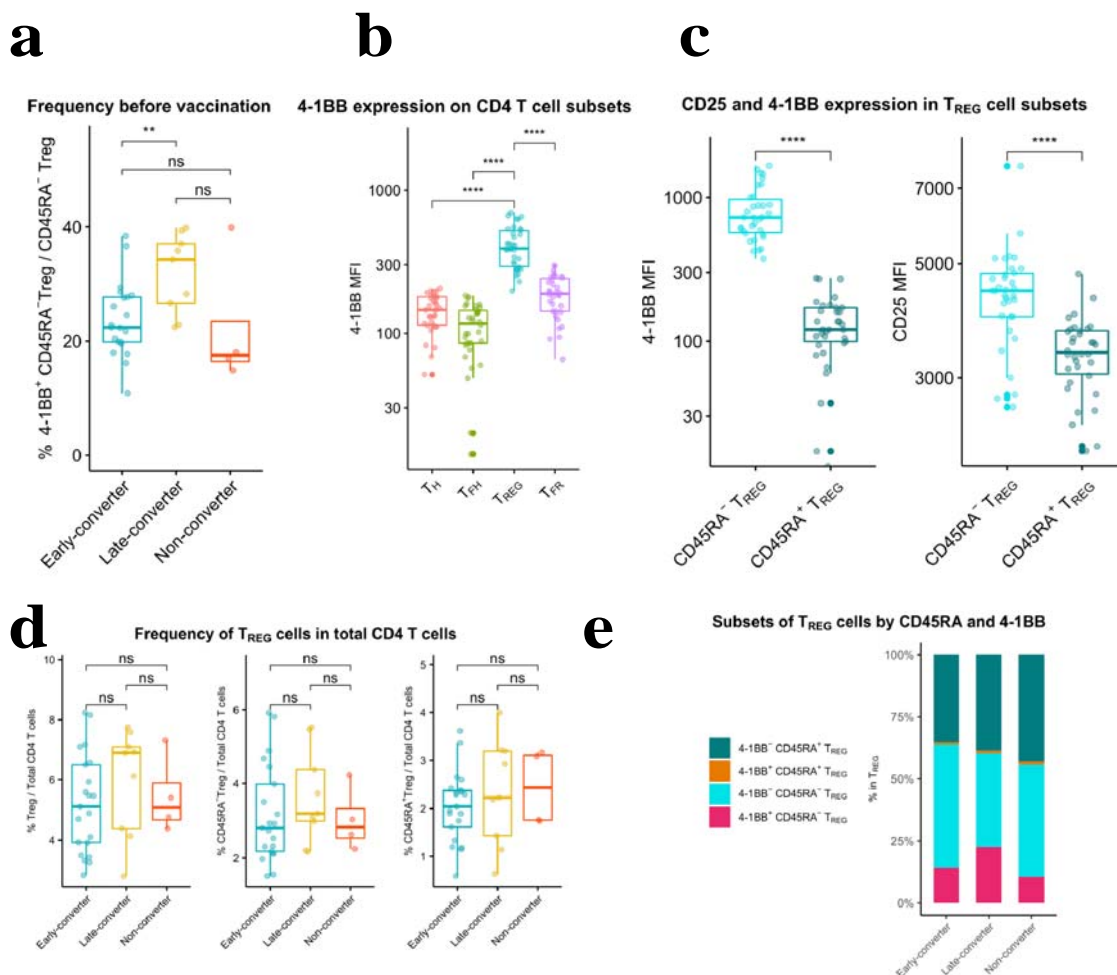
839 group (blue: early-converter, yellow: late-converter, red: non-converter).
840 **c** HBsAg-predictive ratio, \mathbf{R}_{hbs} , when calculated on the memory CD4 TCR β repertoires at day 60.
841 **d** HBsAg-predictive ratio, \mathbf{R}_{hbs} , when calculated on the memory CD4 TCR β repertoires at day 0.
842 **e** Receiver operating characteristic (ROC) curve using \mathbf{R}_{hbs} to differentiate between early-converters and late-
843 converters in a leave-one-out cross validation at day 0. Reported is the area under the curve (AUC) and its 95%
844 confidence interval.
845
846
847
848
849
850
851
852



853
854 **Figure 4. Hepatitis B vaccine induces a vaccine-specific CD40L⁺4-1BB⁻ and CD40L⁻4-1BB⁺**
855 **memory CD4 T cell response in early-converter vaccinees.**

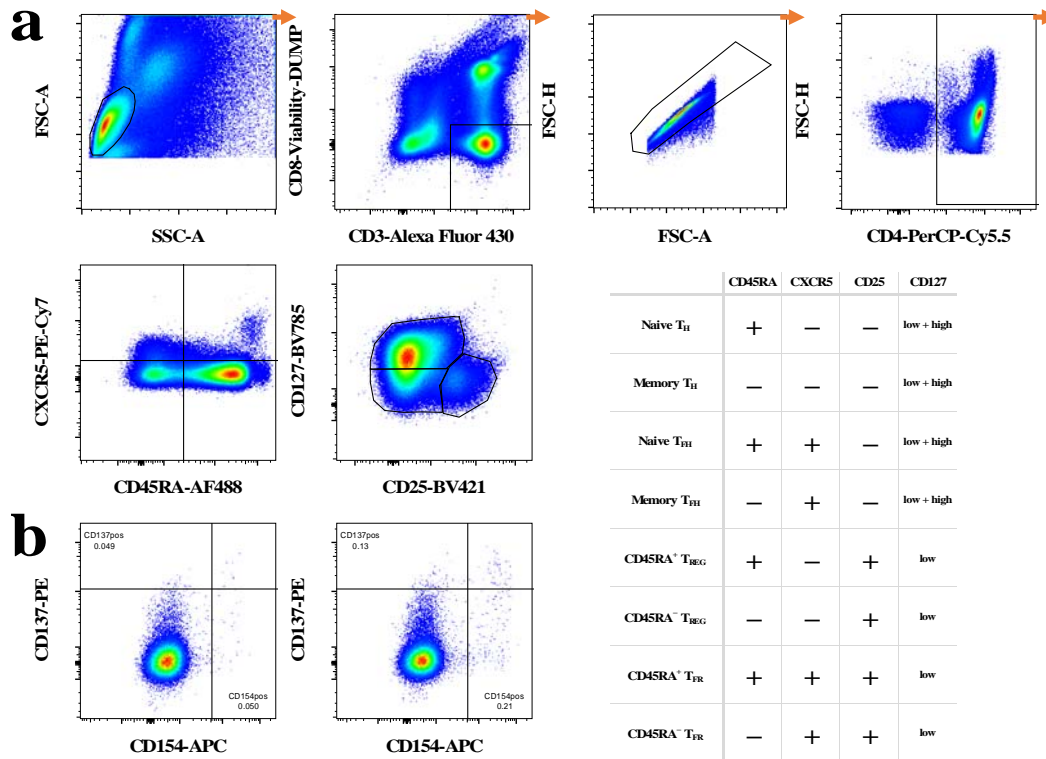
856 PBMCs from vaccinees were stimulated with 2 μ g/ml of the master peptide pool (HBsAg) and assessed for converse
857 expression of 4-1BB and CD40L by flow cytometry on days 0, 60, 180, and 365. Shown is number of of vaccine-
858 specific memory CD4 T cells out of 10^6 memory CD4 T cells after subtraction of responses in negative control.

859 **a** Aggregate analysis from vaccinees (including early, late and non-converters) showing a peak of vaccine-specific
 860 CD40L⁺4-1BB⁻ and CD40L⁻4-1BB⁺ memory CD4 T cell at day 60 (day 60 after 1st dose of the vaccine and day 30
 861 after 2nd dose), declining thereafter. Shown are numbers of vaccine-specific memory CD4 T cells out of 10⁶ memory
 862 CD4 T cells.
 863 **b** Correlation between the difference in antibody titer between day 365 and day 0 and vaccine-specific CD40L⁺4-
 864 1BB⁻ and CD40L⁻4-1BB⁺ memory CD4 T cell at day 60.
 865 **c** Aggregate analysis from early and late-converter vaccinees showing a significant induction of vaccine-specific
 866 CD40L⁺4-1BB⁻ and CD40L⁻4-1BB⁺ memory CD4 T cell in early-converters and lack thereof in late-converters.
 867 **d** Aggregate analysis from early and late-converter vaccinees showing no significant differences in vaccine-specific
 868 CD40L⁺4-1BB⁻ and CD40L⁻4-1BB⁺ memory CD4 T cell at day 0.
 869 **e** Receiver operating characteristic (ROC) curves for R_{hbs} from day 0 data in a leave-one-out cross-validation
 870 compared to the frequency of vaccine-specific CD40L⁺4-1BB⁻ memory CD4 T cell out of 10⁶ memory CD4 T cells
 871 for each vaccinee at time points 60 (AUC = 0.84), 180 (AUC = 0.56) and 365 (AUC = 0.57).
 872 **f** Receiver operating characteristic (ROC) curves for R_{hbs} from day 0 data in a leave-one-out cross-validation
 873 compared to the frequency of vaccine-specific CD40L⁻4-1BB⁺ memory CD4 T cell out of 10⁶ memory CD4 T cells
 874 for each vaccinee at time points 60 (AUC = 0.62), 180 (AUC = 0.56) and 365 (AUC = 0.52).
 875 Wilcoxon signed-rank with unpaired and paired analysis as necessary; statistical significance was indicated with ns
 876 P > 0.05, * P ≤ 0.05, ** P ≤ 0.01, *** P ≤ 0.001, **** P ≤ 0.0001
 877 *r_s*, Spearman correlation coefficient, -1 ≤ *r_s* ≤ 1; *r_s* and *p* value by Spearman's correlation test
 878



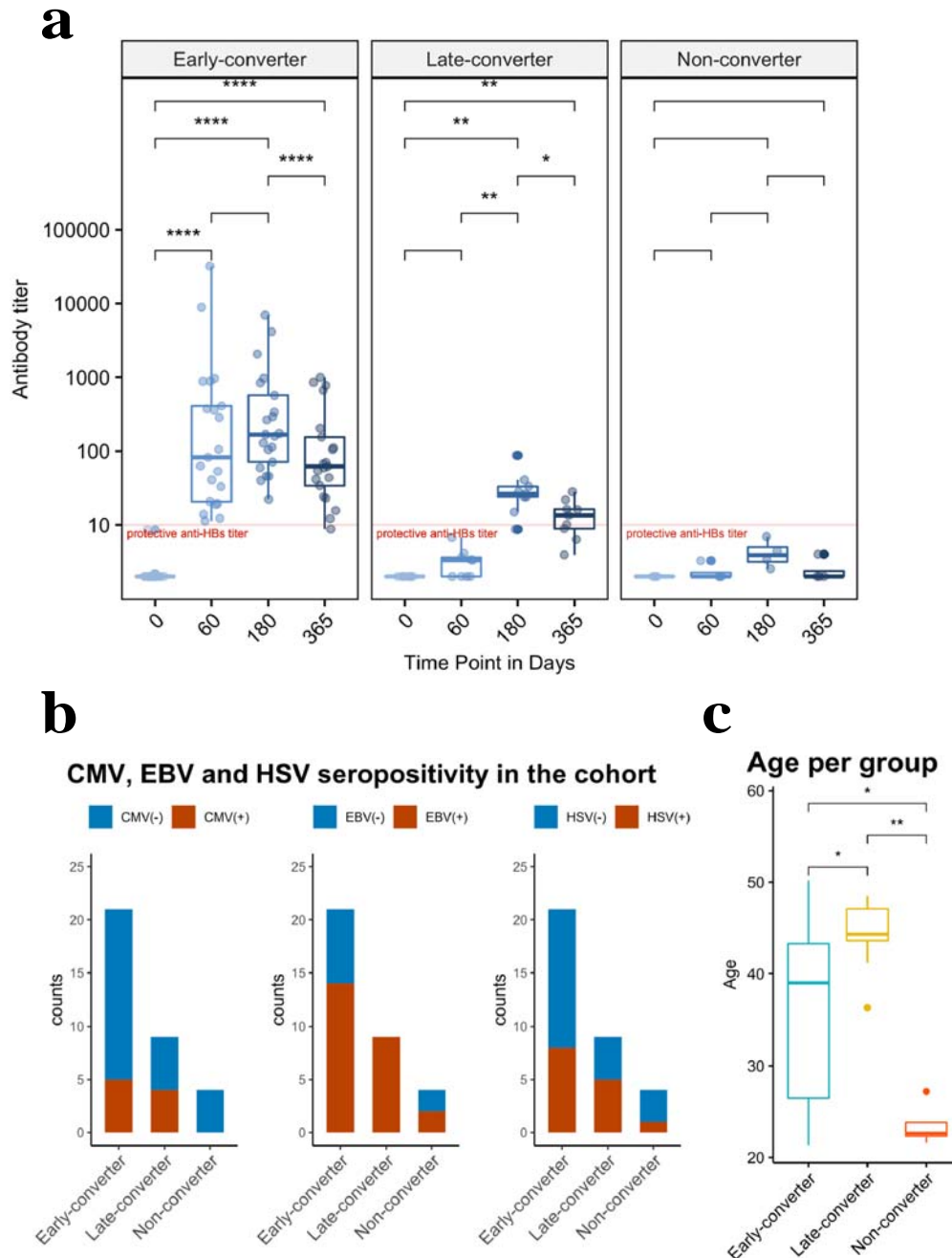
879 **Figure 5. An expanded 4-1BB⁺CD45RA⁻ T_{REG} cells within T_{REG} compartment is a**
 880 **prominent feature in late-converters prior to vaccination.**
 881

882 PBMCs from vaccinees at day 0 (prior to vaccination) were phenotyped for expression of markers of T_{REG}.
 883 **a** Aggregate analysis of 4-1BB⁺CD45RA⁻ T_{REG} within CD45RA⁻ T_{REG} CD4 T cells in early and late and non-
 884 converter vaccinees before vaccination.
 885 **b** Aggregate analysis of the median fluorescence intensity of 4-1BB in T_H, cT_{FH}, T_{REG} and cT_{FR} cells before
 886 vaccination.
 887 **c** Aggregate analysis of the median fluorescence intensity of 4-1BB (left panel) and CD25 (right panel) in CD45RA⁻
 888 T_{REG} and CD45RA⁺ T_{REG} cells before vaccination.
 889 **d** Frequency of T_{REG}, CD45RA⁻ T_{REG} and CD45RA⁺ T_{REG} cells within total CD4 T cells in early, late and non-
 890 converter vaccinees before vaccination.
 891 **e** Composition of T_{REG} compartment as determined by expression of 4-1BB and CD45RA in early, late and non-
 892 converter vaccinees before vaccination.
 893 Wilcoxon signed-rank with unpaired and paired analysis as necessary; statistical significance was indicated with ns
 894 P > 0.05, * P ≤ 0.05, ** P ≤ 0.01, *** P ≤ 0.001, **** P ≤ 0.0001
 895
 896



897
 898 **Figure S1. Gating strategy of ex vivo T cell phenotyping of vaccine-specific T cells.**
 899 **a** Gating strategy started by a lymphocyte gate, followed by gating on viable CD3⁺CD8⁻ T cells. Doublets were
 900 excluded using
 901 doublet discrimination (area against the height of forward scatter pulse) before gating on CD4⁺ T cells. Next,
 902 CD45RA, CXCR5, CD25 and CD127 were used to identify main subsets of CD4 T cells using Boolean gates as
 903 specified in the accompanying table.
 904 **b** Shown an example of gating for CD154 (CD40L) and CD137 (4-1BB) for cells left unstimulated (left) and cells
 905 stimulated with a master peptide pool (right) for an early-converter vaccinee at day 60.
 906

907



908

909

910

Figure S2. Serological memory to hepatitis B vaccine and vaccinee groups within the cohort.

911

912

913

914

915

916

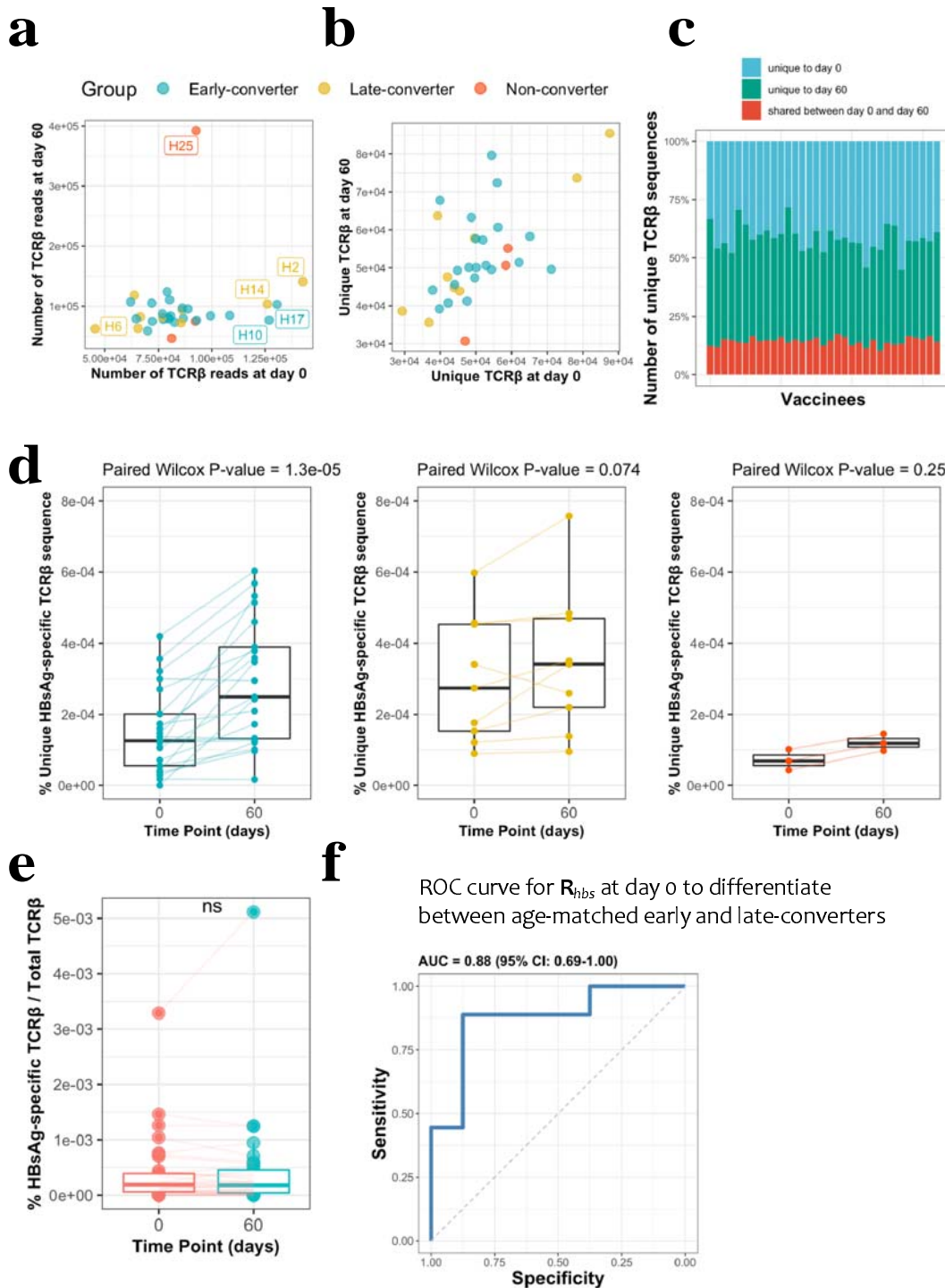
917

918

a Anti-Hepatitis B surface (anti-HBs) titer of vaccinees over four times points, faceted by groups of early, late and non-converters. An anti-HBs titer above 10 IU/ml was considered protective. Early-converters seroconverted at day 60, late-converters seroconverted at day 180 or day 365 and non-converters did not have an anti-HBs titer higher than 10 IU/ml at any of the time points. b CMV, EBV and HSV seropositivity in the three groups of the cohort as determined by serum IgG antibodies to CMV, EBV-VCA, and HSV-1 and 2 using sandwich ELISA. c Age of vaccinees per group.

Wilcoxon signed-rank with unpaired and paired analysis as necessary; statistical significance was indicated with ns $P > 0.05$, * $P \leq 0.05$, ** $P \leq 0.01$, *** $P \leq 0.001$, **** $P \leq 0.0001$

919
920



921
922
923
924
925

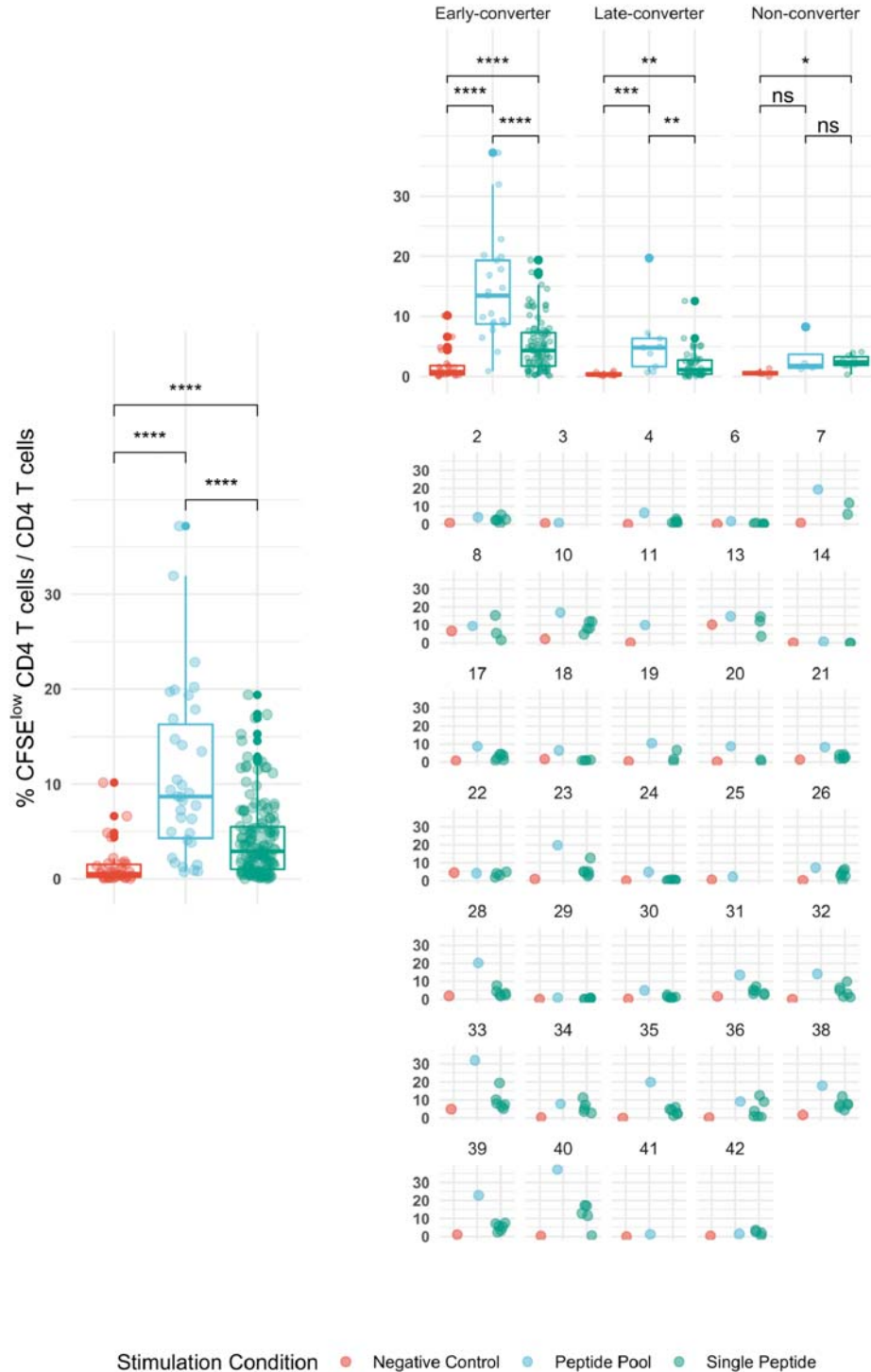
Figure S3. CD4 T cell memory TCRβ repertoire and vaccine-specific TCRβ clonotypes.

a Scatter plot of the DNA-based TCRβ reads for each vaccinee at each time point.

b Scatter plot of number of unique TCRβ amino acid sequences for each vaccinee at each time point, where the shape denotes the response as based on antibody titer.

926 c Overview of unique TCR β amino acid sequences in the memory CD4 T cell repertoire of each vaccinee. The
927 bottom blue bar denotes those TCR sequences that were found at both time points. The green and red bars denote the
928 number of unique TCR sequences at each time point. The total bar height thus represents the total number of unique
929 memory CD4 T cell clonotypes sequences for a specific vaccinee.
930 d Frequency of unique HBsAg-specific TCR β sequences out of total sequenced TCR β sequences between two time
931 points for all vaccinees colored and faceted by group.
932 e Change in frequency of those HBsAg-specific CD4 T cells present at both time points. The (ns) mark denotes a
933 non-significant paired Wilcoxon signed-rank test (p-value = 0.7577).
934 f Receiver operating characteristic (ROC) curve using R_{hbs} to differentiate between age-matched early-converters
935 and late-converters in a leave-one-out cross validation at day 0. Age-matching was accomplished retaining only
936 samples in the age range 40-55. A Wilcoxon test was used to confirm that there was no difference in
937 age distributions between early and late converters (P value = 0.60, mean EC = 44.5y, mean LC
938 45.1y). Diagonal line denotes a random classifier. Reported is the area under the curve (AUC) and its 95%
939 confidence interval.
940
941

In vitro expansion of CD4 T cells (7 days)



942

943

Figure S4. Overview of the results of in vitro expansion experiments.

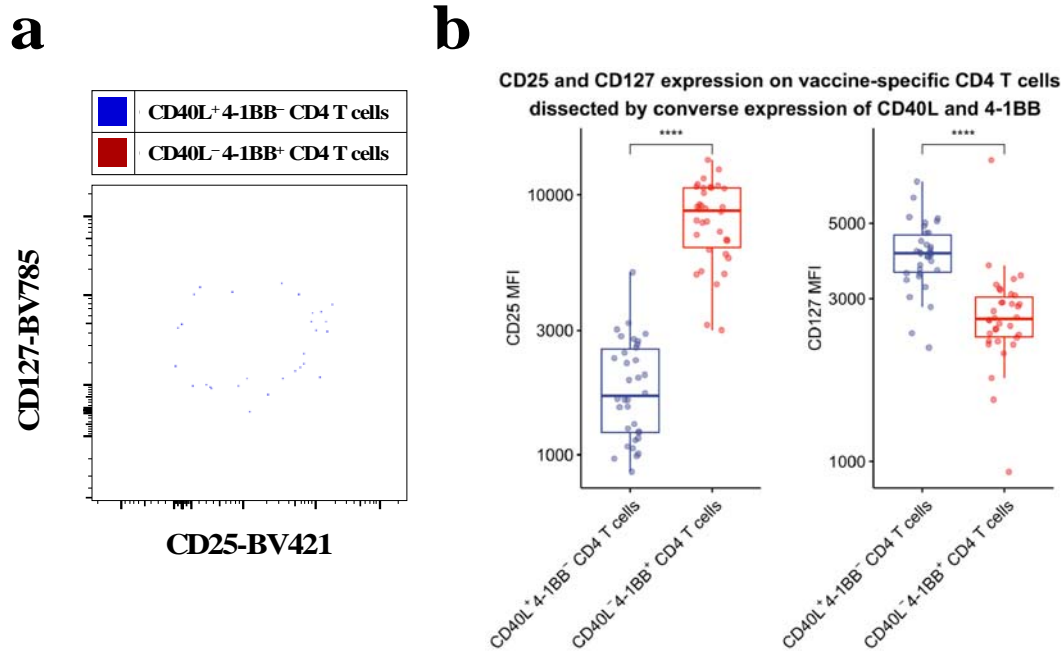
944 Shown is the frequency of CFSE^{low} CD4 T cells out of total CD4 T cells for all vaccinees,

945 vaccinees per group and for each vaccinee. Peripheral blood mononuclear cells from day 60 were

946 labeled with carboxyfluorescein succinimidyl ester (CFSE) and stimulated with a pool of

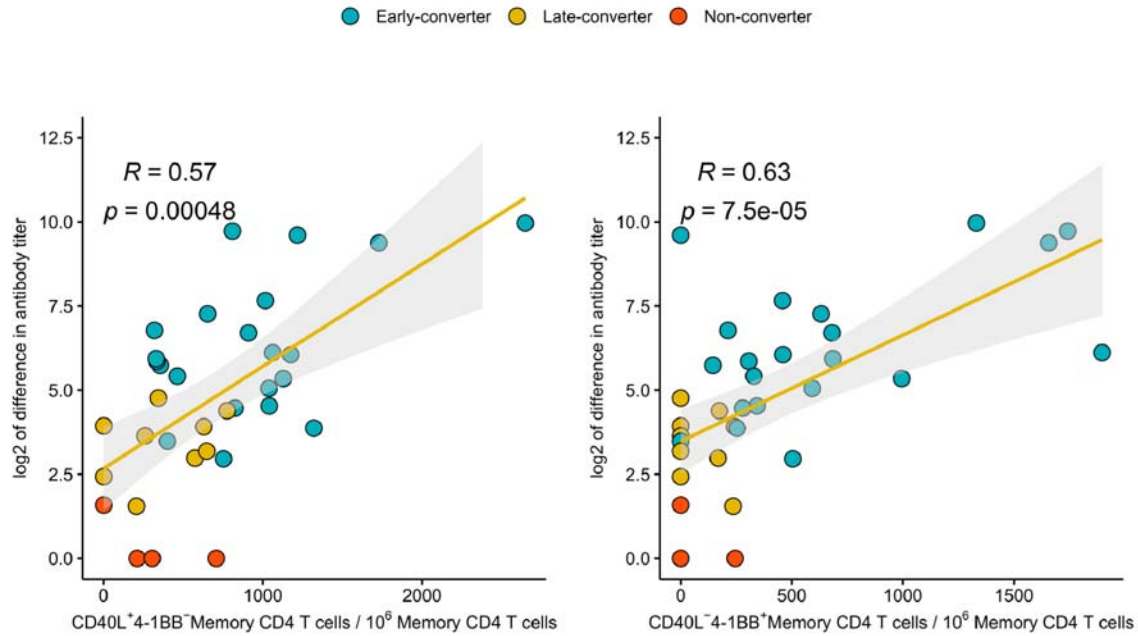
947 peptides spanning hepatitis B (HB) surface antigen (HBsAg) (**Peptide Pool**) and single peptides

948 selected based on epitope mapping of the entire antigen (**Single Peptide**). After day 7 of in vitro
949 expansion, cells were stained with antibodies to surface markers (CD3, CD4 and CD8) that
950 enable gating on viable CD4 T cells. CFSE intensity was used to identify and sort CFSE^{low} cells
951 for TCR repertoire analysis of antigen-specific CD4 T cells.
952



953 **Figure S5. CD40L⁺4-1BB⁻ and CD40L⁻4-1BB⁺ CD4 T cells have a T_{CON} and T_{REG}**
954 **phenotype, respectively.**
955 PBMCs from vaccinees were stimulated with 2 µg/ml of a pool of peptides of HBsAg and
956 assessed for converse expression of 4-1BB and CD40L by flow cytometry. a CD40L⁺4-1BB⁻
957 and CD40L⁻4-1BB⁺ CD4 T cells from day 60 were gated on and then overlaid in a contour plots
958 of CD25 versus CD127 to assess T_{COV} and T_{REG} phenotype. b summary plot of median
959 fluorescence intensity (MFI) of CD25 and CD127 for all vaccinees.
960 Wilcoxon signed-rank with paired analysis; statistical significance was indicated with **** P ≤
961 0.0001
962
963

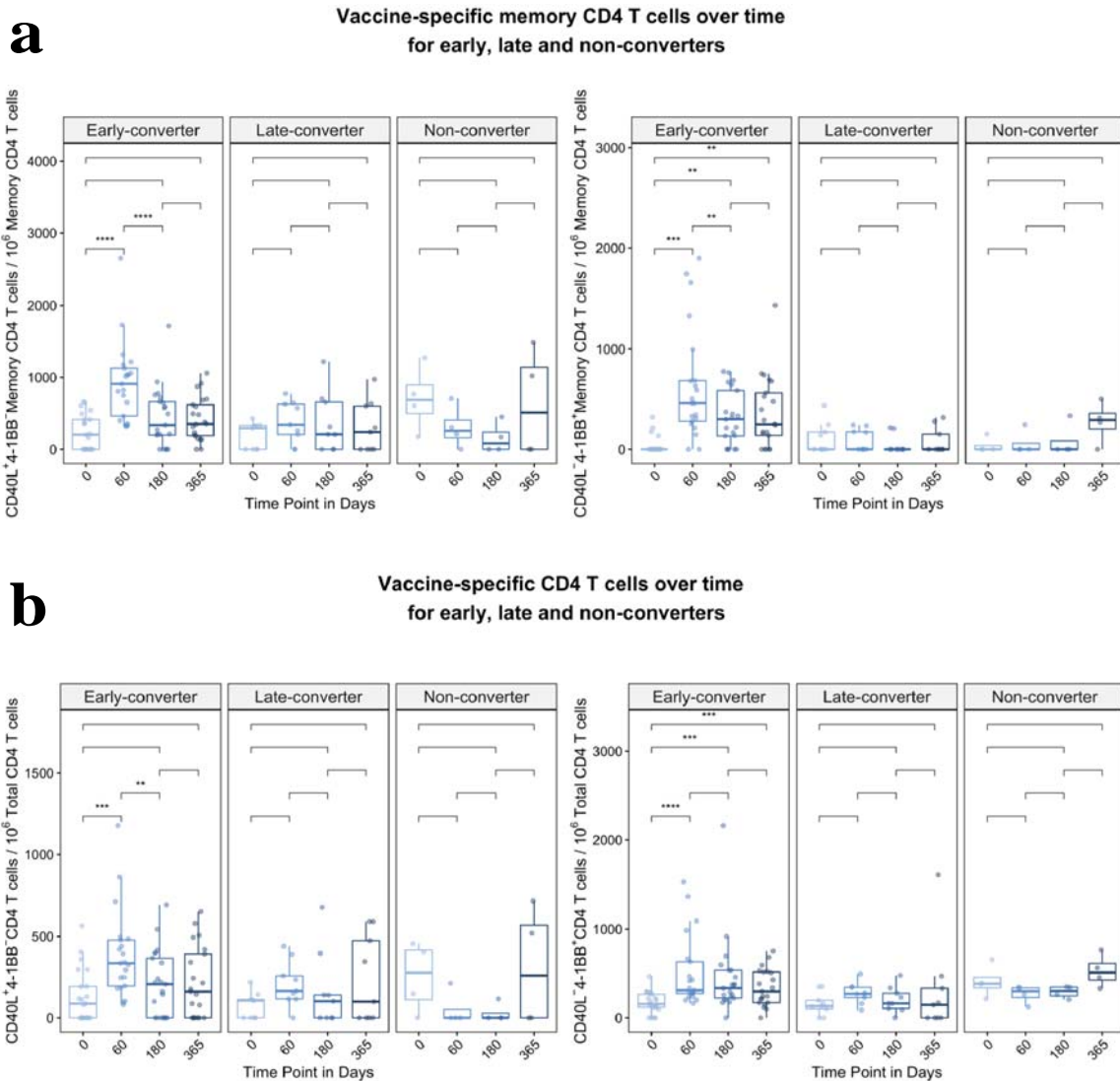
Correlation of vaccine-specific memory CD4 T cells at day 60 and antibody titer difference between day 365 and day 0



964
965
966
967
968
969
970
971

Figure S6. Relationship between serological memory and memory CD4 T cell response to the vaccine.

Correlation between the difference in antibody titer between day 365 and day 0 and vaccine-specific CD40L⁺4-1BB⁻ and CD40L⁻4-1BB⁺ memory CD4 T cell at day 60 colored by vaccinee group and labeled with vaccinee ID. r_s , Spearman correlation coefficient, $-1 \leq r_s \leq 1$; r_s and p value by Spearman's correlation test



972

973

974

Figure S7. Hepatitis B vaccine induces a vaccine-specific CD4 T cell response in early-converter vaccinees.

975

PBMCs from vaccinees were stimulated with 2 $\mu\text{g/ml}$ of a pool of peptides of HBsAg and assessed for converse expression of 4-1BB and CD40L by flow cytometry on days 0, 60, 180, and 365.

976

a Aggregate analysis from early, late and non-converter vaccinees showing a significant induction of vaccine-specific CD40L⁺4-1BB⁻ and CD40L⁺4-1BB⁺ memory CD4 T cell in early-converters and lack thereof in late and non-converters. Shown are numbers of vaccine-specific memory CD4 T cells out of 10⁶ memory CD4 T cells after subtraction of responses in negative control (see Methods for details).

977

b Aggregate analysis from early, late and non-converter vaccinees showing a significant induction of vaccine-specific CD40L⁺4-1BB⁻ and CD40L⁺4-1BB⁺ CD4 T cell in early-converters and lack thereof in late and non-converters. Shown are numbers of vaccine-specific CD4 T cells out of 10⁶ CD4 T cells after subtraction of responses in negative control (see Methods for details).

978

979

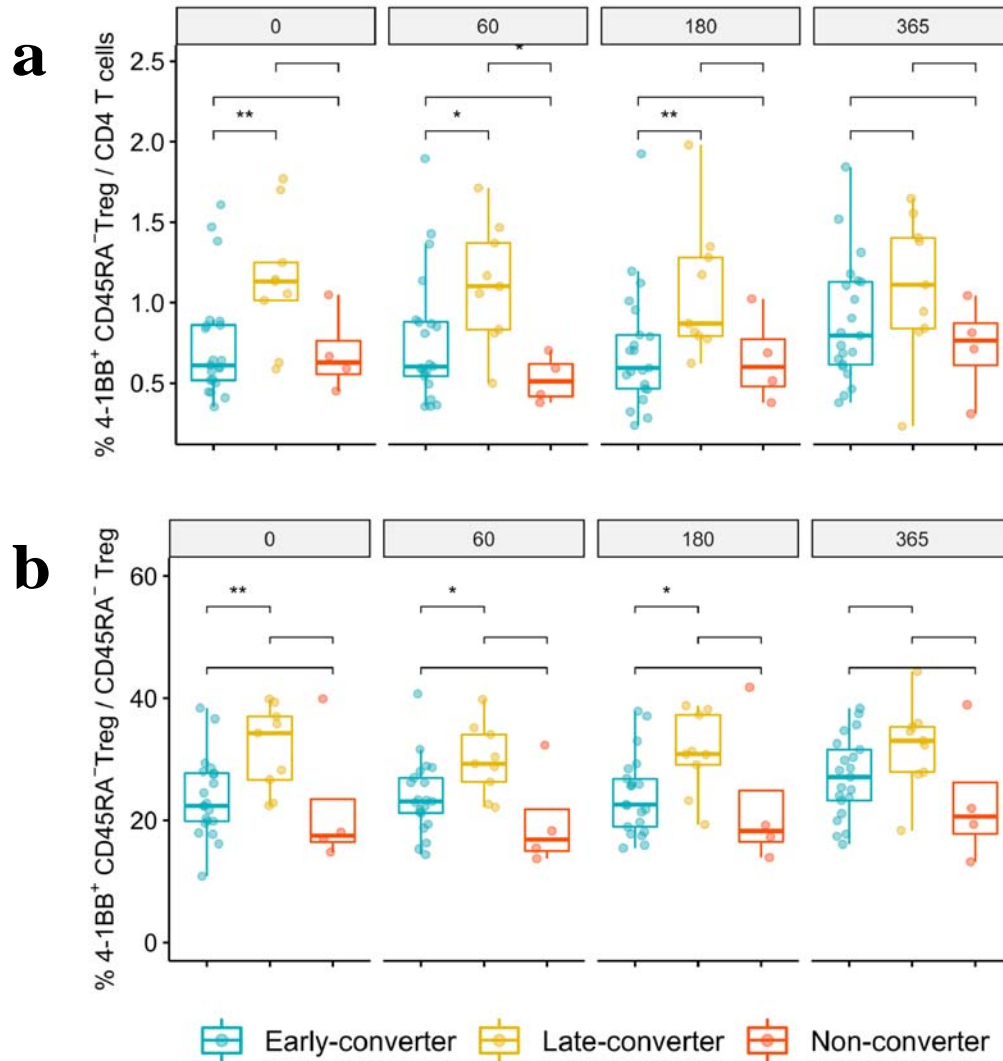
980

981

982

983

984



985
986 **Figure S8. An expanded 4-1BB⁺CD45RA⁻ T_{REG} cells within T_{REG} compartment is a**
987 **prominent feature in late-converters prior to vaccination.**

988 Aggregate analysis of the frequency of 4-1BB⁺CD45RA⁻ T_{REG} within **a** total CD4 T cells and **b** CD45RA⁻ T_{REG}
989 CD4 T cells in early, late and non-converter vaccinees at days 0, 60, 180 and 365.

990 Wilcoxon signed-rank with unpaired and paired analysis as necessary; statistical significance was indicated with ns
991 P > 0.05, * P ≤ 0.05, ** P ≤ 0.01, *** P ≤ 0.001, **** P ≤ 0.0001

992

993 **Supplemental tables**

994 **Supplementary Table 1.**

995 List of 54 single peptides, each 15 AA long with an 11-amino acid overlap spanning the 226 amino acids along the
996 small S protein of hepatitis B (HB) surface antigen (HBsAg)

Peptide No.	15 AA with 11 AA overlap	No. of AA at which the peptide starts
1	MENITSGFLGPLLVL	1
2	TSGFLGPLLVLQAGF	5
3	LGPLLVLQAGFFLLT	9
4	LVLQAGFFLLTRILT	13
5	AGFFLLTRILTIPQS	17
6	LLTRILTIPQSLDSW	21
7	ILTIPQSLDSWWTSL	25
8	PQSLDSWWTSLNFLG	29
9	DSWWTSLNFLGGSPV	33
10	TSLNFLGGSPVCLGQ	37
11	FLGGSPVCLGQNSQS	41
12	SPVCLGQNSQSPTS	45
13	LGQNSQSPTSNSHPT	49
14	SQSPTSNSHPTSCPP	53
15	TSNSHPTSCPPICPG	57
16	SPTSCPPICPGYRWM	61
17	CPPICPGYRWMCLRR	65
18	CPGYRWMCLRRFIIF	69
19	RWMCLRRFIIFLFI	73
20	LRRFIIFLFIILLCL	77
21	IIFLFIILLCLIFLL	81
22	FILLCLIFLLVLLD	85
23	LCLIFLLVLLDYQGM	89
24	FLLVLLDYQGMLPVC	93
25	LLDYQGMLPVCPLIP	97
26	QGMLPVCPLIPGTT	101
27	PVCPLIPGTTTNTG	105
28	LIPGTTTNTGPKCT	109
29	STTTNTGPKCTCTTP	113
30	NTGPKCTCTTPAQGN	117
31	CKTCTTPAQGNMFP	121
32	TTPAQGNMFPSCCC	125
33	QGNSMFPSCCCTKPT	129
34	MFPSCCCTKPTDGN	133
35	CCCTKPTDGNCTCIP	137
36	KPTDGNCTCIPISS	141
37	GNCTCIPISSWAF	145
38	CIPISSWAFACYLW	149
39	PSSWAFACYLWEWAS	153
40	AFACYLWEWASVRF	157
41	YLWEWASVRFWSLS	161
42	WASVRFWSLSLVPF	165
43	RFSWSLSLVPFVQWF	169
44	LSLLVPFVQWVGLS	173

45	VPFVQWVGLSPTVW	177
46	QWVGLSPTVWLSAI	181
47	GLSPTVWLSAIWMMW	185
48	TVWLSAIWMMWYWGP	189
49	SAIWMMWYWGPSLYS	193
50	MMWYWGPSLYSIVSP	197
51	WGPSLYSIVSPFIPL	201
52	LYSIVSPFIPLPIF	205
53	VSPFIPLPIFFCLW	209
54	IPLPIFFCLWVYI	213

997

998

999

1000 **Supplementary Table 2.**

1001 Overview of the single peptides tested for each vaccinee in the CFSE assay

1002

Vaccinee	Gender	Age	Status	peptides_number	single peptides
2	F	43.6	Late-converter	6	51, 35, 50, 34, 54, 38
3	F	48.5	Late-converter	6	53, 5, 37, 49, 1, 33
4	M	47.1	Late-converter	6	21, 20, 5, 53, 4, 52
6	F	44.3	Late-converter	6	23, 39, 7, 21, 37, 5
7	M	38.3	Early-converter	2	17, 33
8	M	43.4	Early-converter	3	47, 41, 42
10	F	33.2	Early-converter	5	49, 1, 33, 41, 9
11	F	39	Early-converter	6	53, 50, 5, 2, 8, 21
13	F	45.9	Early-converter	3	24, 8, 16
14	M	36.3	Late-converter	2	45, 47
17	F	26.5	Early-converter	6	10, 42, 9, 41, 14, 46
18	M	43.3	Early-converter	4	6, 38, 5, 37
19	M	41.3	Early-converter	3	40, 16, 8
20	F	48.7	Early-converter	2	6, 1
21	F	27.2	Non-converter	6	2, 1, 3, 42, 41, 43
22	F	22.3	Early-converter	4	10, 13, 12, 16
23	F	43.9	Late-converter	6	51, 54, 48, 43, 47, 46
24	F	47.7	Late-converter	6	22, 24, 23, 20, 18, 46
25	F	22.6	Non-converter	6	29, 30, 28, 21, 22, 20
26	F	41.2	Late-converter	6	23, 47, 17, 41, 7, 49
28	F	41.7	Early-converter	6	54, 38, 52, 36, 40, 39
29	M	39.5	Early-converter	6	7, 47, 6, 1, 23, 46
30	F	45.1	Late-converter	6	22, 46, 54, 19, 20, 43
31	M	32.4	Early-converter	6	54, 38, 49, 33, 53, 37
32	F	31.4	Early-converter	6	7, 4, 1, 6, 31, 28
33	F	41	Early-converter	6	1, 41, 7, 5, 47, 45
34	M	22.5	Early-converter	5	7, 4, 5, 2, 6
35	F	50.2	Early-converter	6	46, 45, 47, 22, 21, 23
36	F	23.2	Early-converter	6	54, 47, 46, 39, 48, 38
38	F	23.2	Early-converter	6	37, 34, 33, 35, 5, 2
39	M	45.8	Early-converter	6	51, 50, 53, 49, 35, 34
40	F	21.3	Early-converter	5	33, 38, 37, 39, 40
41	M	21.6	Non-converter	6	23, 22, 7, 6, 17, 1
42	M	22.7	Non-converter	4	1, 33, 25, 41

1003

1004

1005